Title

CoQ10 production in Schizosaccharomyces pombe is increased by reduction of glucose levels or deletion of pka1

Author(s)

Ikuhisa Nishida, Kazumasa Yokomi, Kouji Hosono, Kazuhiro Hayashi, Yasuhiro Matsuo, Tomohiro Kaino & Makoto Kawamukai

Journal

Applied Microbiology and Biotechnology volume 103, pages4899–4915(2019)

Published

27 April 2019

URL

https://doi.org/10.1007/s00253-019-09843-7

CoQ_{10} production in *Schizosaccharomyces pombe* is increased by reduction of glucose levels or deletion of *pka1*

Ikuhisa Nishida[1], Kazumasa Yokomi[1], Kouji Hosono[1], Kazuhiro Hayashi[1], Yasuhiro Matsuo[1, 2], Tomohiro Kaino[1, 2], & Makoto Kawamukai[1, 2]

[1]Department of Life Sciences, Faculty of Life and Environmental Sciences, Shimane University, 1060 Nishikawatsu, Matsue 690-8504, Japan.

[2]Institute of Agricultural and Life Sciences, Academic Assembly, Shimane University, 1060 Nishikawatsu, Matsue 690-8504, Japan.

Corresponding author: Makoto Kawamukai: E-mail: kawamuka@life.shimane-u.ac.jp. Telephone/Fax: 81-852-32-6587, Fax: 81-852-32-6092.

Key words: Coenzyme Q; ubiquinone; *Schizosaccharomyces pombe*; cAMP/PKA pathway

Abstract

Coenzyme Q (CoQ) is an essential component of the electron transport system that produces ATP in nearly all living cells. CoQ_{10} is a popular commercial food supplement around the world, and demand for efficient production of this molecule has increased in recent years. In this study, we explored CoQ_{10} production in the fission yeast *Schizosaccharomyces pombe*. We found that CoQ_{10} level was higher in stationary phase than in log phase, and that it increased when the cells were grown in a low concentration of glucose, in maltose, or in glycerol/ethanol medium. Because glucose signaling is mediated by cAMP, we evaluated the involvement of this pathway in CoQ biosynthesis. Loss of Pka1, the catalytic subunit of cAMP-dependent protein kinase, increased production of CoQ_{10}, whereas loss of the regulatory subunit Cgs1 decreased production. Manipulation of other components of the cAMP-signaling pathway affected CoQ_{10} production in a consistent manner. We also found that glycerol metabolism was controlled by the cAMP/PKA pathway. CoQ_{10} production by the *S. pombe* Δ*pka1* reached 0.98 mg/g dry cell weight in medium containing a non-fermentable carbon source [2% glycerol (w/v) and 1% ethanol (w/v) supplemented with 0.5% casamino acids (w/v)], 2-fold higher than the production in wild-type cells under normal growth conditions. These findings demonstrate that carbon source, growth phase, and the cAMP-signaling pathway are important factors in CoQ_{10} production in *S. pombe*.

Introduction

Coenzyme Q (CoQ), also called ubiquinone (Crane et al. 1957; Morton 1958), is a component of the mitochondrial electron transport chain that participates in aerobic respiration in eukaryotes and most prokaryotes. CoQ consists of a quinone ring and a hydrophobic isoprenoid side chain that has the all-trans configuration of a certain length of isoprene units. CoQ is the most abundant prenylquinone in living cells (Kawamukai 2018). The quinone moiety is reduced to form $CoQH_2$ (ubiquinol), which functions as a lipid-soluble antioxidant. A CoQ-producing organism possesses one type of CoQ as a main product, which is classified according to the length of the isoprenoid side chain (Kawamukai 2002). For example, *Schizosaccharomyces pombe* and *Homo sapiens* predominantly produce CoQ_{10}, with ten isoprene units; *Mus musculus* and *Arabidopsis thaliana* produce CoQ_9; *Escherichia coli* produces CoQ_8; and *Saccharomyces cerevisiae* produces CoQ_6 (Kawamukai 2009). The side chain length of CoQ is defined by a species-specific polyprenyl diphosphate synthase (Okada et al. 1996; Okada et al. 1998). The biosynthetic pathway for the complete conversion of *p*-hydroxybenzoate (PHB) to CoQ consists of at least eight steps (Fig. 1). After the polyprenyl diphosphate is synthesized, it is transferred to PHB by Coq2 (Ppt1) (PHB-polyprenyl diphosphate transferase). Prenylated PHB is subjected to the following modifications in the six-membered ring: three hydroxylations by Coq6, Coq7, and a still-unidentified enzyme(s), *O*-methylations by Coq3, *C*-methylation by Coq5, and decarboxylation by an unknown enzyme(s) (Kawamukai 2016). In eukaryotes, this pathway has been most comprehensively studied to date in *S. cerevisiae* and *S. pombe* (Tran and Clarke 2007; Hayashi et al. 2014). At least ten genes (*COQ1–COQ9*, and *COQ11*) in *S. cerevisiae* (Allan et al. 2015) and 11 genes (*dps1*, *dlp1*, *ppt1*, *coq3–coq9*, and *coq11*) in *S. pombe* are required for CoQ biosynthesis (Uchida et al. 2000; Miki et al. 2008; Kawamukai 2018). However, the functions of the *COQ4*, *COQ8*, *COQ9*, and *COQ11* genes have not yet been clearly resolved, and moreover, the pathway upstream of PHB synthesis is only partially understood (Payet et al. 2016).

CoQ_{10} (or $CoQ_{10}H_2$) has attracted a great deal of attention in recent years as a medicine, health food, and a cosmetic, and the demand for CoQ_{10} has risen accordingly. Several approaches have been used to improve fermentative production of CoQ_{10} by modifying various CoQ-related metabolic pathways in bacterial and yeast mutants (Lee et al. 2017). *S. pombe* is an ideal platform to produce CoQ_{10} because we have a detailed understanding of the metabolic pathways involved in CoQ_{10} synthesis, as well as tools for genetically modifying this species (Hayashi et al. 2014). In a previous study, we were

partially successful in metabolic engineering of CoQ_{10} biosynthesis in *S. pombe* (Moriyama et al. 2015; Moriyama et al. 2017). CoQ_{10} production was increased by overexpression of *E. coli ubiC* (encoding chorismate lyase), *E. coli aroF*(*fbr*) (encoding 3-deoxy-D-arabino-heptulosonate 7-phosphate synthase), or *S. cerevisiae thmg1* (encoding truncated HMG-CoA reductase) (Moriyama et al. 2015). However, *S. pombe* strains overexpressing individual CoQ biosynthetic genes did not enhance CoQ_{10} production more than 10%, in most cases due to growth inhibition.

In *S. pombe*, glucose signaling is mainly mediated by the cAMP/PKA pathway, which consists of the seven-transmembrane G protein–coupled receptor Git3, heterotrimeric G protein alpha subunit Gpa2, beta subunit Git5, gamma subunit Git11, adenylate cyclase Cyr1, regulatory subunit Cgs1, and catalytic subunit Pka1 (Maeda et al., 1994; Devoti et al. 1991; Kawamukai et al. 1991; Welton et al. 2000; Gupta et al. 2011). *S. pombe* PKA is involved in multiple cellular processes, including sexual development (Kawamukai et al. 1991), oxidative and salt stress (Roux et al. 2006; Matsuo et al. 2008), and calcium homeostasis (Matsuo and Kawamukai 2017).

In this study, we investigated CoQ_{10} production in *S. pombe* at various growth stages, under different glucose or other carbon conditions, and in mutants in genes related to the PKA pathway. We found that glucose concentration, carbon source, and PKA were critical for CoQ_{10} production in *S. pombe*.

Material and methods

Yeast strains and media

The *S. pombe* strains used in this study are listed in Tables S1 and S2; the genotype of the parental strain in Table S2 is *h⁻ leu1-32 ura4-D18* (Bimbó et al. 2005). The strains PR109 (FY33782) and PR110 (FY33783) are available in NBRP-Yeast, Japan.

Standard yeast culture media and genetic methods were used (Alfa 1993; Petersen et al. 2016; Ito et al. 1983). *S. pombe* strains were grown in complete YES medium (0.5% yeast extract; 3% glucose; and 225 mg/L each of adenine sulfate, leucine, uracil, histidine, and lysine hydrochloride). Glucose concentration or the carbon source in YES was changed depending on the purpose of the experiment. Non-fermentable carbon source medium [2% glycerol (w/v) and 1% ethanol (w/v) with or without 0.5% casamino acid (w/v)] was prepared. For synthetic medium, pombe minimal medium (PM) with 75 mg/L uracil was used as necessary. The promoter and polyadenylation signal of the thiamine-repressible gene *nmt1* of *S. pombe* have been used to construct

the vector pREP3X and to over-express the *rst2* or *rst2* (C2H2Δ) gene (Maundrell 1990; Takenaka et al. 2018). Wild-type cells were transformed with pREP3X, pREP3X-Rst2, or pREP3X-Rst2(C2H2Δ) and selected on PMU containing 10 μM thiamine. For *rst2* overexpression, transformants were grown on PMU containing 0.15 μM thiamine for 1 day at 30°C. After three washes with distilled pure water, cells were transferred onto PMU without thiamine and incubated for 2 days at 30°C.

Growth test

S. pombe cells were pre-cultured in 10 mL of YES liquid medium for 1 day at 30°C. The pre-culture was inoculated into a larger volume of medium, and the main culture was grown for the indicated periods of time. For growth assays, cells were counted on a cell counter (Sysmex CDA-500 or CDA-1000B).

CoQ extraction and measurement

S. pombe cells were grown in YES liquid media containing various carbon sources at 30°C. At the indicated times, cells were harvested, and CoQ was extracted as described previously (Hayashi et al. 2014). The CoQ crude extract was analyzed by normal-phase thin layer chromatography (TLC) with authentic CoQ_6 or CoQ_{10} standards. Normal-phase TLC was conducted on a Kieselgel 60 F_{254} plate (Merck Millipore) and developed with benzene. The plate was viewed under UV illumination, the CoQ band was collected, and the sample was extracted with hexane/isopropanol (1:1, v/v). Samples were dried and solubilized in ethanol. Purified CoQ was subjected to high-performance liquid chromatography on a Shimadzu HPLC Class *VP* series equipped with a reverse phase YMC-Pack ODS-A column (YMC). Ethanol was used as the mobile phase at a flow rate of 1.0 mL/min, and detection was performed by monitoring absorption at 275 nm.

Antibody

To immunochemically detect CoQ biosynthetic proteins, each peptide (Dlp1, CDIEAKQALMEIANSVSK; Coq3, CYNPLKQQWTLDKPGSSG; Coq4, CNKMLVDKTGREILKDKPRM; Coq5, CSVGLRRSKKTPYYDSGR; Coq8, CKELFSGMLKHYAD) was used to immunize rabbits. Peptides and rabbit polyclonal antisera were prepared by Sigma-Aldrich. The specificity of antisera against each CoQ biosynthetic protein (Dlp1, Coq3, Coq4, Coq5, and Coq8) was assessed by western blot analysis in wild-type and individual *dlp1* and *coq* deletion strains. The corresponding bands were absent in all gene disruptants. However, we saw a background protein overlapping with Coq3 when antisera against the Coq3 peptide was used (Fig. S5).

Preparation of cell lysates and detection of CoQ biosynthetic proteins by immunoblotting

S. pombe cell lysates were prepared as described (Masai et al. 1995). Each of the *S. pombe* cells (PR109 (W. T.), PR110 (W. T.), YMP40 (Δ*cgs1*), YMP177 (Δ*cgs1*), YMP36 (Δ*pka1*), and YMP179 (Δ*pka1*)) was inoculated into 55 mL YES main cultures (starting concentration, ~1×10^5 cells/mL) and incubated with rotation at 30°C for 2 days and harvested. Lysate proteins were separated by SDS-PAGE, after which western blot analysis was performed using an ECL detection system (GE Healthcare). Rabbit polyclonal antibodies against CoQ biosynthetic proteins (Dlp1, diluted 1:1000; Coq3, diluted 1:1000; Coq4, diluted 1:1000; Coq5, diluted 1:500; Coq8, diluted 1:1000) and against PSTAIRE (Cdc2, diluted 1:1000) were purchased from Sigma and Santa Cruz Biotechnology, respectively. Horseradish peroxidase–conjugated anti-rabbit IgG antibody (Promega) was used as secondary antibody (diluted 1:2000). These antibodies were dissolved in Can Get Signal immunostain Immunoreaction Enhancer Solution (TOYOBO).

Microarray analysis

Pre-cultures of PR110 (wild-type), YMP41 (Δ*cgs1*), or YMP37 (Δ*pka1*) cells were inoculated into 50 mL main cultures (starting concentration, ~1×10^5 cells/mL) and incubated with rotation at 30°C. Aliquots of cells were taken after 8 hours (log phase). The cells were harvested at 4°C. Total RNA for transcriptomic analysis was isolated using the RNeasy Mini Kit (Qiagen). After RNase A cleanup, double-strand cDNA was prepared using the Invitrogen SuperScript Double-strand cDNA Synthesis Kit. Purified cDNA was labeled using the NimbleGen One-color Labeling Kit, and the labeled products were precipitated with isopropanol and dried. The dried pellets were dissolved in NimbleGen Sample Tracking Control. NimbleGen Hybridization Mix was prepared according to the NimbleGen Hybridization Kit protocol. The hybridization mix was incubated on an array (*Schizosaccharomyces pombe* (4-Plex Array) v2 (A6187-00-02, NimbleGen)) in an Agilent Microarray Hybridization Oven for 16–20 hours at 42°C, and then the microarray was washed with wash buffer in a slide container at 42°C. The hybridized array was scanned on a Microarray Scanner (Agilent G2565BA), and fluorescence intensities were extracted using the Feature Extraction Software (Agilent). The microarray data were deposited in NCBI's Gene Expression Omnibus with the accession number GSE125392.

Data and statistical analyses

All experiments were performed more than three times, and the average values and standard deviation (SD) were calculated. Data from control and target sample(s) were compared using the two-sample t test in Microsoft Excel. p-values <0.05 were considered statistically significant.

Reproducibility

All experiments were conducted at least twice to confirm the reproducibility of the results.

Results

S. pombe CoQ_{10} contents change as a function of growth stage

Because *S. pombe* holds promise as a microorganism in which to efficiently produce CoQ_{10}, we sought to identify conditions that affect CoQ_{10} production. To determine how CoQ_{10} production changes during growth, we evaluated the productivity of CoQ_{10} after cells were grown in 3% glucose containing YES complete medium for various periods of time (Fig. 2). CoQ_{10} production was assessed as total production per volume (gray bar) and amount per cell (white bar). The CoQ_{10} level per cell was lower in early log phase (8–16 hours) than at the starting point. During mid-log (20–24 hours) and late log (30–36 hours) growth phase, CoQ_{10} level per volume and per cell gradually increased in a time-dependent manner. In stationary (48–72 hours) and death phase (120–240 hours), the total amount of CoQ_{10} kept increasing, but CoQ_{10} level per cell did not increase as much. We found that CoQ_{10} is continually synthesized during prolonged incubation and is approximately 2-fold higher in stationary and death phase than in mid-log phase. Because stationary phase occurs after glucose is exhausted, we hypothesized that glucose is the key component that affects the CoQ_{10} level in *S. pombe*.

Lower glucose concentration increased CoQ_{10} content

The results described above suggested that the glucose concentration in the medium affects the CoQ_{10} level in *S. pombe*. To test this hypothesis, we evaluated CoQ_{10} levels at 12 different glucose concentrations (0.02%, 0.05%, 0.1%, 0.2%, 0.5%, 1%, 2%, 3%, 5%, 7%, 10%, and 20%) in YES medium after 48 hours cultivation (Fig. 3a). We started at 0.02% glucose because no cell growth was observed at lower glucose concentrations in YES. Total CoQ_{10} level per cell (white bar) tended to increase in low cell number (diamond) such as at 0.02 to 0.1 % glucose concentration when the cell growth was not sufficient. As we predicted, CoQ_{10} levels per cell were 2.2- and 1.6- fold higher in 0.02 and 0.05% glucose respectively than in standard YES (3% glucose). At higher glucose concentrations, CoQ_{10} per cell tended to decrease. This effect was much clearer in comparisons of CoQ_{10} levels in early stationary phase under higher glucose (10% or 20%). In the higher glucose (20%) medium, the cells produced 2.3-fold less CoQ_{10} than in 3% glucose (Fig. 3b). Consistent with the importance of glucose concentration, a longer (7 day) batch cultivation in 10% glucose YES produced a higher level of CoQ_{10} than cells grown in 3% glucose (Table 2), because glucose concentration eventually decreased over the long incubation period. Thus, the intracellular level of CoQ_{10} was higher under glucose limitation and lower under high-glucose conditions.

The cAMP-dependent protein kinase (PKA) pathway is involved in CoQ_{10} production

In light of our observation that glucose concentration affects CoQ_{10} production in *S. pombe*, we hypothesized that protein kinase A participating in the response to carbon sources may be involved in CoQ_{10} biosynthesis. To explore this idea and also test the possible involvement of other kinases, we obtained 87 single deletion mutants of non-essential kinases including Pka1 (Table S2 and Fig. S1) and examined the amount of CoQ_{10} in each. CoQ_{10} level varied among these 87 kinase deletion mutants; in particular, the Δ*pka1* (MBY1787) strain exhibited a significant increase. To validate this finding, we checked other Δ*pka1* mutants from different sources. Indeed, Δ*pka1* strains JZ633, YMP36, YMP37, and YMP179 also contained higher levels of CoQ_{10} than the wild type (Fig. S2; data for JZ633 are not shown).

PKA is the signaling kinase of the cAMP/PKA pathway, which senses glucose concentration and transduces that information to downstream effectors (Fig. 4a). When glucose is abundant, it is sensed by the receptor Git3, and then Gpa2 is released to activate Cyr1 (adenylate cyclase), which generates cAMP. Binding of cAMP to Cgs1 releases Pka1 to phosphorylate multiple target proteins (Kawamukai et al. 1991; Hoffman 2005; Gupta et al. 2010a). Thus, the observation that both reduced levels of glucose and deletion of *pka1* increase production of CoQ_{10} is consistent with the known role of Pka1.

When we tested other mutants related to the PKA pathway, we found that the Δ*git3* (YMP43), Δ*gpa2* (YMP39), and Δ*cyr1* (YMP28) strains increased production of CoQ_{10}, and Δ*cgs1* (YMP40) significantly decreased production of CoQ_{10} (Fig. 4b). We checked other Δ*cgs1* mutants from different sources (YMP40, YMP41, and YMP177), and all contained lower levels of CoQ_{10} than the wild-type strain (Fig. S2). Because deletion of the *cgs1* gene has the opposite effect from deletion of the *pka1* gene, we concluded that activation of the PKA pathway negatively affects CoQ_{10} production.

To further elucidate the role of Pka1 in the biosynthesis of CoQ_{10}, we investigated the involvement of the transcription factor Rst2, which is controlled by Pka1. To clarify the involvement of Rst2 in CoQ_{10} biosynthesis, we measured the CoQ_{10} levels in PR109 (wild-type), YMP36 (Δ*pka1*), YMP130 (Δ*rst2*), or YMP220 (Δ*pka1* Δ*rst2*) cells (Fig. 5a). The CoQ_{10} level in Δ*rst2* cells was similar to that in the wild-type strain, whereas the Δ*pka1* Δ*rst2* strain contained about 1.2-fold more CoQ_{10}. These results suggest that Pka1 plays a role in CoQ biosynthesis in both Rst2-dependent and -independent manners. To demonstrate the effect of overexpression of *rst2* on CoQ_{10} production, we transformed a wild-type strain (PR110) with pREP3X (vector control),

pREP3X-Rst2 (*nmt1-rst2*), or pREP3X-Rst2(C2H2Δ) [*nmt1-rst2* (C2H2Δ), which lacks a DNA binding domain], and tested their levels of CoQ_{10}. Although overexpression of *rst2* and its C2H2Δ mutant resulted in strong growth inhibition, as observed previously (Takenaka et al. 2018), the CoQ_{10} content per cell number increased (Fig. 5b). A similar trend in CoQ_{10} level was observed after a shorter incubation (1 day) following inoculation of a larger number of cells (Fig. S3).

Maltose or a combination of glycerol and ethanol as a carbon source increases CoQ_{10} content

Glucose is the most preferred carbon source in yeasts and other organisms. When *S. pombe* cells are grown in medium containing higher levels of glucose, they metabolize glucose predominantly through glycolysis, and release ethanol into the medium. By contrast, under glucose-limited conditions, cells change their metabolism from fermentation to respiration. There is a threshold glucose concentration that governs the respiration-dependency of *S. pombe* proliferation (Takeda et al. 2015). Based on this observation, it is conceivable that the amount of CoQ_{10} could be increased by culture in a medium lacking glucose or containing a non-fermentable carbon source.

Maltose is a disaccharide consisting of two units of glucose joined with an α(1→4) bond. In *S. pombe*, maltose is degraded by the secretory maltase Agl1 (Kato et al. 2013), which is only secreted after glucose limitation. In support of our hypothesis, CoQ_{10} level per volume was 1.45-fold higher in maltose medium than in glucose medium after a 7 days incubation (Fig. 6a). Incubation of wild-type cells for 60 hours in maltose medium decreased the CoQ_{10} level per volume relative to glucose medium, while CoQ_{10} levels per volume were similar after 80 hours of incubation (Fig. 6b). Moreover, CoQ_{10} level per cell was 5-fold higher after 48 hours in maltose medium than after 20 hours in glucose medium, although the cell number under both conditions was similar (1×10^7 cells/mL) (Fig. S4). Both growth and CoQ_{10} production in maltose were lower in the Δ*pka1* strain (Fig. 6b and Fig. S4), possibly because the cAMP/PKA pathway regulates maltose metabolism.

Involvement of the cAMP/PKA pathway in glycerol metabolism

We next sought to determine how the CoQ_{10} level is controlled by PKA. To this end, we first examined the protein levels of CoQ-synthesizing enzymes. For this purpose, we raised antibodies against various proteins involved in CoQ synthesis (Saiki et al. 2003; Hayashi et al. 2014), and successfully obtained antibodies against Dlp1, Coq3, Coq4, Coq5, and Coq8. When we assessed the levels of these proteins in wild-type, Δ*cgs1*, and

303 Δ*pka1* strains by western blotting, using anti-PSTAIRE (Cdc2) as a loading control, we
304 observed no clear differences in Coq protein levels among the strains tested (Fig. 7).
305 However, among the five proteins we examined, we noticed the level of Coq4 was lower
306 in the Δ*cgs1* strain and higher in Δ*pka1* strains than in the wild-type. These results suggest
307 that the cAMP/PKA pathway affects some of CoQ protein expressions.
308 We next explored the possibility that the cAMP/PKA pathway affects the
309 expression of the genes involved in CoQ_{10} synthesis and other related metabolic pathways.
310 To that end, we performed microarray analyses on wild-type, Δ*cgs1*, and Δ*pka1* strains.
311 Relative to the wild type, expression of 156 and 11 genes was altered in Δ*pka1* and Δ*cgs1*,
312 respectively (Table 1). However, CoQ biosynthetic gene expression did not change in
313 Δ*pka1* (not listed in Table 1). Thus, the microarray analysis did not provide a clear
314 indication that the CoQ biosynthetic gene expressions were controlled by the cAMP/PKA
315 pathway.
316 Interestingly, expression of *gld1*, which is required for glycerol metabolism, and
317 *dak2*, which encodes dihydroxyacetone kinase, was elevated more than 3-fold in the
318 Δ*pka1* strains (Table 1). We confirmed the significant upregulation of *gld1* in Δ*pka1*
319 (YMP37) relative to the wild type (PR110) and Δ*cgs1* (YMP41) by quantitative real time
320 PCR (data not shown).
321 To evaluate the role of *pka1* in utilization of non-fermentable carbon source, we
322 grew PR109 (wild type), YMP40 (Δ*cgs1*), and YMP36 (Δ*pka1*) in non-fermentable
323 carbon source medium (2% glycerol and 1% ethanol) and compared their growth (Fig.
324 8a). The Δ*pka1* strain grew better than the wild type, whereas the Δ*cgs1* strain grew more
325 slowly. This result suggested that a non-fermentable carbon source might affect CoQ_{10}
326 productivity; accordingly, we measured the CoQ_{10} level in YES medium containing
327 glycerol and ethanol. In non-fermentable carbon source medium, the CoQ_{10} level was
328 higher in Δ*pka1* than in the wild type, but lower in Δ*cgs1* (Fig. 8b). These results indicate
329 that PKA controls glycerol utilization in addition to CoQ_{10} level. We observed further
330 increases in CoQ_{10} level in YES medium containing glycerol and ethanol as carbon
331 sources and in YES medium containing glycerol, ethanol, and casamino acids compared
332 with in glucose medium (Fig. 8c). We measured dry cell weight (DCW) in representative
333 conditions and assessed CoQ_{10} productivity as shown in Table 2. The CoQ_{10} productivity
334 varied greatly depending on the type of carbon sources and the cultivation period.
335 Glycerol medium tended to increase CoQ_{10} productivity to a greater extent than glucose
336 medium in both the wild type (PR110) and the Δ*pka1* strain (YMP179). The highest level
337 of CoQ_{10} was 175 μg/10^9 cells, corresponding to 0.98 mg/g-DCW (Table 2).
338

Discussion

In this study, we investigated CoQ_{10} productivity in the fission yeast *S. pombe*, a promising microorganism for CoQ_{10} production due to accumulated knowledge regarding its metabolic pathways and the availability of suitable genetic tools. We examined the effects of medium, growth condition, and genes on CoQ_{10} productivity. We found that CoQ_{10} accumulated to higher levels in the stationary and death phase than in log phase. At stationary phase, yeast cells have already consumed the glucose in the medium (Hamburger and Kramhøft 1982), and glucose deprivation halts cell growth. Upon consumption of glucose in the medium, *S. pombe* undergo transient cell-cycle arrest specifically at G2 phase, extending their chronological lifespan (Masuda et al. 2016). Consistent with the higher productivity of CoQ_{10} at stationary phase, we observed higher CoQ_{10} levels under low-glucose condition (0.02–0.05%). When glucose is limiting, cell growth is restricted; consequently, cells experience a shorter log phase. When energy productivity declines following a decrease in glucose concentration, cells shift to higher respiratory activity by increasing the level of CoQ_{10} to compensate. Intriguingly, cells continue CoQ_{10} synthesis, and degradation of the compound barely occurs even when cells stop growing or enter death phase (Fig. 2).

The cAMP/PKA pathway (Fig. 4a) is a key signaling mechanism that responds to the glucose level (Hoffman 2005; DeVoti et al. 1991). The intracellular cAMP level decreases when the extracellular glucose concentration is low, and under this condition Pka1 remains inactivated due to binding with Cgs1 (Gupta et al. 2010b). Conversely, when the external glucose concentration is higher, intracellular cAMP levels rise, and binding of cAMP to Cgs1 releases Pka1 to be activated. Therefore, glucose concentration in the medium and Pka1 activity are inter-related. Inactivation of Pka1 under lower glucose and *pka1* (*git3*, *gpa2*, or *cyr1*) gene deletion create similar situations within the cell. We found that deficiency of *pka1* results in higher production of CoQ_{10} (Fig. 4b), whereas by contrast, loss of Cgs1 decreased the CoQ_{10} level. In Δ*rst2*, the CoQ_{10} level did not differ from that in the wild-type strain. However, Δ*pka1* Δ*rst2* contained a lower level of CoQ_{10} than Δ*pka1*, implying that Pka1 requires Rst2 for its execution of the role. In this case, both transcriptional and non-transcriptional control are conceivable, but we do not have a clear answer about how Pka1 affects the production of CoQ_{10}. By analogy to CoQ biosynthesis in *S. cerevisiae*, it is possible that some Coq biosynthetic proteins are regulated by phosphorylation: in budding yeast, PKA or PKC (Protein kinase C) is involved in phosphorylation of three residues of *S. cerevisiae* Coq7, which controls oxygenase activity (Martín-Montalvo et al. 2011). Substitution of Ser20, Ser28, and Thr32 of Coq7 with alanine increases the CoQ_6 level by ~2.6-fold. However, although a

phosphorylation-mediated mechanism is involved in *S. cerevisiae* CoQ biosynthesis, it remains to be seen whether such regulation occurs in *S. pombe*.

It has been shown that *S. cerevisiae* produced a CoQ_6 intermediate, 3,4-dihydroxy-5-hexaprenylbenzoate (3,4-DHHB) and lowered CoQ_6 production when grown in 10% glucose, but not in 1% glucose media. Accumulation of 3,4-DHHB was inhibited by addition of cAMP (Sippel et al. 1983). Accumulation of another intermediate compound, DMQ_6, has been shown when *S. cerevisiae* was grown in non-fermentable YPG medium (Padilla et al. 2009). Decreases of CoQ level in high glucose media are commonly found in both *S. cerevisiae* and *S. pombe*. But, we do not see any clear accumulation of CoQ_{10} intermediate(s) when cells were grown in high glucose or non-fermentable media in *S. pombe*. Further detail analysis is necessary for clearing this point.

Consistent with the importance of glucose level as a determinant of CoQ_{10} productivity, we observed a higher level of CoQ_{10} when maltose was used as the carbon source. *S. pombe* secretes the extracellular maltase Agl1, which hydrolyzes maltose into glucose, and can thus use maltose as a carbon source. Transcription of *agl1* is dependent on Atf1 and Pcr1 (Kato et al. 2013). *S. pombe* cannot take up maltose directly; instead, the glucose produced by the activity of Agl1 is brought into the cell via hexose transporters. Secretion of Agl1 takes a relatively long time, causing cells to experience a lower level of glucose, and consequently to accumulate a higher level of CoQ_{10}. In non-fermentable carbon source medium [2% glycerol (w/v) and 1% ethanol (w/v) with or without 0.5% casamino acid], the CoQ_{10} level was higher than in glucose medium (Fig. 6b), likely due to a mechanism similar to that operating under low-glucose condition. Moreover, addition of casamino acid to 2% glycerol (w/v)/1% ethanol (w/v) effectively promoted cell growth in non-fermentable carbon source medium, suggesting that casamino acid accelerates glycerol metabolism in both the wild type and Δ*pka1*.

When we assessed the levels of five Coq proteins in the wild type, Δ*pka1*, and Δ*cgs1* strains by western blotting, we observed Coq4 was downregulated in Δ*cgs1* and upregulated in Δ*pka1* (Fig. 7). This suggest that cAMP/PKA pathway affects some of CoQ protein expressions, but a detailed investigation is necessary to confirm this. Moreover, the expression of the *dps1*, *dlp1*, *ppt1*, *coq3–coq9*, and *coq10* genes was not altered in the Δ*pka1* or Δ*cgs1* strains, as determined by microarray analyses (data not shown). This result suggest that genes related to CoQ biosynthesis are not regulated by Pka1 or Cgs1 at the transcriptional level in *S. pombe*.

Our observation that the CoQ_{10} level increased in the Δ*pka1* cells suggested that the electron transfer system in the mitochondria might be activated in this mutant. Indeed, Δ*pka1* grew faster in medium containing a non-fermentable carbon source (2% glycerol

411 + 1% ethanol) (Fig. 8), which predicts that the cAMP/PKA pathway regulates glycerol
412 metabolism. The glycerol metabolic enzyme of *S. pombe* Gld1, known as glycerol
413 dehydrogenase, synthesizes dihydroxyacetone (DHA); Dak1 and Dak2 dihydroxyacetone
414 kinases synthesize dihydroxyacetone phosphate (DHAP), which connects the pathway to
415 glycolysis (Matsuzawa et al. 2010). Gld1, Dak1, and Dak2 undergo different types of
416 transcriptional control by the transcription factors Scr1, Tup11, and Tup12, respectively
417 (Janoo et al. 2001; Hoffman et al. 1991). Moreover, the wild type and Δ*pka1* exhibited
418 slightly diauxic growth in medium containing glycerol and ethanol as a carbon source,
419 whereas Δ*cgs1* did not (Fig. 8a), implying that cells metabolize ethanol before glycerol
420 at each proliferation of wild type and Δ*pka1* cells. Our microarray analyses showed that
421 expression of genes involved in the glycerol metabolism system, including *gld1*, was
422 elevated in Δ*pka1*, suggesting that proliferation in glycerol and ethanol medium is
423 necessary to promote expression of *gld1* downstream of the cAMP/PKA pathway.
424 Catabolite repression is an idea that may explain higher CoQ_{10} levels under low-glucose
425 or non-fermentable carbon source condition. Microarray analysis in Δ*pka1* cells suggest
426 the involvement of PKA in catabolite repression through upregulating the expression of
427 the genes involve sugar fermentation such as glycerol metabolic enzyme *Gld1*, alfa-
428 galactosidase Mel1 and alfa-glucosidases (Gto1, Gto2, Agl1) (Table 1). The upregulation
429 of hexose transporters Ght1, Ght3 and Ght4 in Δ*pka1* cells were also observed as a
430 response to elevate hexose transportation through the glucose sensing PKA pathway. In
431 fact, these hexose transporter genes are upregulated by shifting from high glucose to low
432 glucose media (Saito et al. 2015). We also noticed many genes were upregulated in Δ*pka1*
433 cells, while a few were affected in Δ*cgs1* cells. This indicates that sensing of lowered
434 glucose level as a role of the PKA pathway is mechanistically important than sensing
435 higher glucose. We think sensing lower level of glucose by the PKA pathway widely
436 affects cellular metabolisms, and as a consequence of not well explainable effects, CoQ_{10}
437 level becomes high in Δ*pka1* cells.
438 In summary, CoQ_{10} is produced in *S. pombe* at high levels under low-glucose
439 conditions or in a Δ*pka1* strain, but its levels decrease in higher glucose during log phase
440 (Fig. S6). Prolonged incubation of *S. pombe* cells tends to increase the CoQ_{10} level, and
441 genetic modification of the cAMP/PKA pathway is useful for over-production of CoQ_{10}.
442 We succeeded in producing 0.98 mg of CoQ_{10} per DCW (g) at most (Table 2) when
443 glycerol/ethanol medium was used. In order to achieve much higher CoQ_{10} production up
444 to 10 mg / dry cell weight as observed in some other microorganisms (Kawamukai 2016;
445 Lee et al. 2017), further investigation will be necessary. The findings in this study pave

446 the way for applying *S. pombe* to the industrial production of CoQ_{10}.
447
448
449 **Acknowledgments**
450 *S. pombe* kinase gene deletion mutants were kindly provided by M. Balasubramanian.
451 Δ*pka1* (JZ633) was provided by M. Yamamoto. The authors also thank Dr. T. Nakagawa,
452 H. Okazaki, and all other members of the laboratory for helpful discussions and support.
453
454
455 **Compliance with Ethical Standards**
456
457 **Funding**
458 This work was partly supported by a grant-in-aid from the Ministry of Education, Culture,
459 Sports, Science, and Technology of Japan [#25660059, #17H03806, and #24380056] to
460 M.K., [#15K07360 and #18K05393] to T.K., [#18K14377] to I.N., [#18K05438] to Y.M.,
461 and by the Science and Technology Research Promotion Program for Agriculture,
462 Forestry, Fisheries, and Food Industry [#957613] to M.K. The authors thank the faculty
463 of Life and Environmental Sciences in Shimane University for help in financial supports
464 for publishing this report.
465

466 **Conflict of interest**

467 The authors declare that they have no conflict of interest.

468

469 **Ethical approval**

470 This article does not contain any studies with human participants or animals.

471
472
473 **References**
474
475 Alfa C. (1993) Experiments with fission yeast: a laboratory course manual. Cold Spring
476 Harbor (NY): Cold Spring Harbor Laboratory Press.
477

Allan CM, Awad AM, Johnson JS, Shirasaki DI, Wang C, Blaby-Haas CE, Merchant SS, Loo JA, Clarke CF. (2015) Identification of Coq11, a new coenzyme Q biosynthetic protein in the CoQ-synthome in *Saccharomyces cerevisiae*. J. Biol. Chem. 290:7517-7534

Bimbó A, Jia Y, Poh SL, Karuturi RK, den Elzen N, Peng X, Zheng L, O'Connell M, Liu ET, Balasubramanian MK, Liu J. (2005) Systematic deletion analysis of fission yeast protein kinases. Eukaryot. Cell 4:799-813

Cohen A, Kupiec M, Weisman R. (2014) Glucose activates TORC2-Gad8 protein via positive regulation of the cAMP/cAMP-dependent protein kinase A (PKA) pathway and negative regulation of the Pmk1 protein-mitogen-activated protein kinase pathway. J. Biol. Chem. 289:21727-21737

Crane FL, Hatefi Y, Lester RL, Widmer C. Isolation of a quinone from beef heart mitochondria. (1957) Biochim. Biophys. Acta. 25:220-221

DeVoti J, Seydoux G, Beach D, McLeod M. (1991) Interaction between *ran1*$^{+}$ protein kinase and cAMP dependent protein kinase as negative regulators of fission yeast meiosis. EMBO J. 10:3759-3768

Gupta DR, Paul SK, Oowatari Y, Matsuo Y, Kawamukai M. (2011a) Complex formation, phosphorylation, and localization of protein kinase A of *Schizosaccharomyces pombe* upon glucose starvation. Biosci. Biotechnol. Biochem. 75:1456–1465

Gupta DR, Paul SK, Oowatari Y, Matsuo Y, Kawamukai M. (2011b) Multistep regulation of protein kinase A in its localization, phosphorylation and binding with a regulatory subunit in fission yeast. Curr. Genet. 57:353-365

Hayashi K, Ogiyama Y, Yokomi K, Nakagawa T, Kaino T, Kawamukai M. (2014) Functional conservation of coenzyme Q biosynthetic genes among yeasts, plants, and humans. PLoS One 9:e99038

Hirota K, Hoffman CS, Ohta K. (2006) Reciprocal nuclear shuttling of two antagonizing Zn finger proteins modulates Tup family corepressor function to repress chromatin remodeling. Eukaryot. Cell 5:1980-1989

Hoffman CS, Winston F. (1991) Glucose repression of transcription of the *Schizosaccharomyces pombe fbp1* gene occurs by a cAMP signaling pathway. Genes Dev. 5:561-571

Hoffman CS. (2005) Glucose sensing via the protein kinase A pathway in *Schizosaccharomyces pombe*. Biochem. Soc. Trans. 33:257-260

Hamburger K, Kramhøft B (1982) Respiration and fermentation during growth and starvation in the fission yeast, *Schizosaccharomyces pombe*. Carlsberg Res. Commun. 47: 405-411

Ito H, Fukuda Y, Murata K, Kimura A. (1983) Transformation of intact yeast cells treated with alkali cations. J. Bacteriol. 153:163-168

Janoo RT, Neely LA, Braun BR, Whitehall SK, Hoffman CS. (2001) Transcriptional regulators of the *Schizosaccharomyces pombe fbp1* gene include two redundant Tup1p-like corepressors and the CCAAT binding factor activation complex. Genetics 157:1205-1215

Kawamukai M, Ferguson K, Wigler M, Young D. (1991) Genetic and biochemical analysis of the adenylyl cyclase of *Schizosaccharomyces pombe.* Cell Regul. 2:155–164

Kawamukai M, (2002) Biosynthesis, bioproduction, and novel roles of ubiquinone. J. Biosci. Bioeng. 94:511-517

Kawamukai M. (2009) Biosynthesis and bioproduction of coenzyme Q10 by yeasts and other organisms. Biotechnol. Appl. Biochem. 53:217–226

Kawamukai M. Biosynthesis of coenzyme Q in eukaryotes. (2016) Biosci. Biotechnol. Biochem. 80:23–33

Kawamukai M. Biosynthesis and applications of prenylquinones. (2018) Biosci. Biotechnol. Biochem. 82:963-977

549 Kato H, Kira S, Kawamukai M (2013) The Transcription Factors Atf1 and Pcr1 Are
550 Essential for Transcriptional Induction of the Extracellular Maltase Agl1 in Fission Yeast.
551 PLoS One 8: e80572. doi: 10.1371/journal.pone.0080572
552
553 Lee SQ, Tan TS, Kawamukai M, Chen ES (2017) Cellular factories for coenzyme Q10
554 production. Microb. Cell Fact. 16:39
555
556 Masai H, Miyake T, Arai K. (1995) *hsk1*$^{+}$, a *Schizosaccharomyces pombe* gene related to
557 *Saccharomyces cerevisiae* CDC7, is required for chromosomal replication. EMBO J. 14:
558 3094-3104.
559
560 Maeda T, Watanabe Y, Kunitomo H, Yamamoto M. (1994) Cloning of the *pka1* gene
561 encoding the catalytic subunit of the cAMP-dependent protein kinase in
562 *Schizosaccharomyces pombe.* J. Biol. Chem. 269:9632-9637
563
564 Masuda F, Ishii M, Mori A, Uehara L, Yanagida M, Takeda K, Saitoh S. (2016) Glucose
565 restriction induces transient G2 cell cycle arrest extending cellular chronological lifespan.
566 Sci. Rep. 6:19629
567
568 Matsuo Y, Mcinnis B, Marcus S. (2008) Regulation of the subcellular localization of
569 cyclic AMP-dependent protein kinase in response to physiological stresses and sexual
570 differentiation in the fission yeast *Schizosaccharomyces pombe*. Eukaryot. Cell 7:1450-
571 1459
572
573 Matsuo Y, Kawamukai M. (2017) cAMP-dependent protein kinase involves calcium
574 tolerance through the regulation of Prz1 in *Schizosaccharomyces pombe.* Biosci.
575 Biotechnol. Biochem. 81:231-241
576
577 Matsuzawa T, Ohashi T, Hosomi A, Tanaka N, Tohda H, Takegawa K. (2010) The *gld1*$^{+}$
578 gene encoding glycerol dehydrogenase is required for glycerol metabolism in
579 *Schizosaccharomyces pombe*. Appl. Microbiol. Biotechnol. 87:715-727
580
581 Martín-Montalvo A, González-Mariscal I, Padilla S, Ballesteros M, Brautigan DL, Navas
582 P, Santos-Ocaña C. (2011) Respiratory-induced coenzyme Q biosynthesis is regulated by
583 a phosphorylation cycle of Cat5p/Coq7p. Biochem. J. 440:107-114
584

585 Miki, R., Saiki, R., Ozoe, Y., Kawamukai, M. (2008) Comparison of a *coq7* deletion
586 mutant with other respiration-defective mutants in fission yeast. FEBS J. 275:5309-5324
587
588 Mitchell P. (1961) Coupling of phosphorylation to electron and hydrogen transfer by a
589 chemi-osmotic type of mechanism. Nature 191:144-148
590
591 Moriyama D, Hosono K, Fujii M, Washida M, Nanba H, Kaino T, Kawamukai M. (2015)
592 Production of CoQ10 in fission yeast by expression of genes responsible for CoQ10
593 biosynthesis. Biosci. Biotechnol. Biochem. 79:1026-1033
594
595 Moriyama D, Kaino T, Yajima K, Yanai R, Ikenaka Y, Hasegawa J, Washida M, Nanba
596 H, Kawamukai M. (2017) Cloning and characterization of decaprenyl diphosphate
597 synthase from three different fungi. Appl. Microbiol. Biotechnol. 101:1559-1571
598
599 Morton RA. (1958) Ubiquinone. Nature 182:1764-1767
600
601 Maundrell K (1990) *nmt1* of fission yeast. A highly transcribed gene completely
602 repressed by thiamine. J. Biol. Chem. 265:10857-10864
603
604 Okada K, Suzuki K, Kamiya Y, Zhu X, Fujisaki S, Nishimura Y, Nishino T, Nakagawa
605 T, Kawamukai M, Matsuda H. (1996) Polyprenyl diphosphate synthase essentially
606 defines the length of the side chain of ubiquinone. Biochim. Biophys. Acta. 1302:217-
607 223
608
609 Okada K, Kainou T, Matsuda H, Kawamukai M. (1998) Biological significance of the
610 side chain length of ubiquinone in *Saccharomyces cerevisiae*. FEBS Lett. 431:241-244
611
612 Padilla S, Tran UC, Jiménez-Hidalgo M, López-Martín JM, Martín-Montalvo A,
613 Clarke, CF. Navas P, Santos-Ocaña C. (2009) Hydroxylation of demethoxy-Q6
614 constitutes a control point in yeast coenzyme Q6 biosynthesis. Cell Mol. Life Sci. 66:
615 173-186
616
617 Payet LA, Leroux M, Willison JC, Kihara A, Pelosi L, Pierrel F. (2016) Mechanistic
618 Details of Early Steps in Coenzyme Q Biosynthesis Pathway in Yeast. Cell Chem. Biol.
619 23:1241-1250
620

621 Petersen J, Russell P. (2016) Growth and the environment of *Schizosaccharomyces*
622 *pombe*. Cold Spring Harb Protoc. 2016(3); pdb top079764. doi: 10.1101/pdb.top079764
623
624 Roux AE, Quissac A, Chartrand P, Ferbeyre G, Rokeach LA. (2006) Regulation of
625 chronological aging in *Schizosaccharomyces pombe* by the protein kinases Pka1 and Sck2.
626 Aging Cell 5:345-357
627
628 Saiki R, Nagata A, Uchida N, Kainou T, Matsuda H, Kawamukai M. (2003) Fission yeast
629 decaprenyl diphosphate synthase consists of Dps1 and the newly characterized Dlp1
630 protein in a novel heterotetrameric structure. Eur. J. Biochem. 270:4113-4121
631
632 Saitoh S, Mori A, Uehara L, Masuda F, Soejima S, Yanagida M. (2015) Mechanisms of
633 expression and translocation of major fission yeast glucose transporters regulated by
634 CaMKK/phosphatases, nuclear shuttling, and TOR. Mol. Biol. Cell. 26:373-386
635
636 Sippel CJ., Goewert RR, Slachman FN, Olson RE. (1983) The regulation of ubiquinone-
637 6 biosynthesis by *Saccharomyces cerevisiae*. J. Biol. Chem. 258:1057-1061
638
639 Takeda K, Starzynski C, Mori A, Yanagida M. (2015) The critical glucose concentration
640 for respiration-independent proliferation of fission yeast, *Schizosaccharomyces pombe*.
641 Mitochondrion 22:91-95
642
643 Takenaka K, Tanabe T, Kawamukai M, Matsuo Y. (2018) Overexpression of the
644 transcription factor Rst2 in *Schizosaccharomyces pombe* indicates growth defect, mitotic
645 defects, and microtubule disorder. Biosci. Biotechnol. Biochem. 82:247-257
646
647 Tran UC, Clarke CF. (2007) Endogenous synthesis of coenzyme Q in eukaryotes.
648 Mitochondrion 7(Suppl):S62–71
649
650 Uchida N., Suzuki K., Saiki R., Kainou T., Tanaka K., Matsuda H Kawamukai M. (2000)
651 Phenotypes of fission yeast defective in ubiquinone production due to disruption of the
652 gene for p-hydroxybenzoate polyprenyl diphosphate tranferase. J. Bacteriol. 182:6933-
653 6939
654
655 Welton RM, Hoffman CS. (2000) Glucose Monitoring in Fission Yeast via the *gpa2* Gα,
656 the *git5* Gβ and the *git3* Putative Glucose Receptor. Genetics. 156:513-521

Figure Legends

Fig. 1 Overview of the CoQ biosynthetic pathway in *S. pombe*. The biosynthetic pathway that converts PHB into CoQ in *S. pombe* consists of eight steps. Decaprenyl diphosphate, which is synthesized by decaprenyl diphosphate synthase (Dps1 + Dlp1), is transferred to PHB by PHB-decaprenyl diphosphate transferase [Ppt1 (Coq2)], and then seven modifications of the aromatic ring are performed in CoQ biosynthesis. DHB, 3-decaprenyl-4-hydroxybenzoate; DPP, decapentenyl diphosphate; FPP, farnesyl diphosphate; IPP, isopentenyl diphosphate; PHB, *p*-hydroxybenzoate.

Fig. 2 *S. pombe* CoQ_{10} production during different growth phases. *S. pombe* cells were pre-cultivated in 15 mL of YES medium for 1 day, inoculated into 850 mL of YES medium at ~1×10^5 cells/mL, and cultivated with rotation at 30°C. At the indicated time points, 50–150 mL of culture was harvested, and CoQ_{10} was extracted and analyzed. Gray bars show CoQ_{10} content per 50 mL of medium. White bars show CoQ_{10} level per 1×10^9 cells. Diamonds show cell number. Ten micrograms of CoQ_6 was used as an internal standard. Data are means ± SD of three measurements. Asterisks on bars denote statistically significant differences (** $p<0.01$; * $p<0.05$) relative to the 48 hours time point (Student's t test).

Fig. 3 Effect of glucose concentration in YES on CoQ_{10} production. Yeast were pre-cultivated in 15 mL of YES (3% glucose) medium for 1 day, washed twice with distilled pure water, inoculated at ~1×10^5 cells/mL into 55 mL of YES medium containing different concentrations of glucose, and then cultured for 48 hours (a) or 24 hours (b) with rotation at 30°C. CoQ_{10} was extracted and analyzed. Gray bars show CoQ_{10} content per 50 mL of medium, and white bars show CoQ_{10} normalized against cell number. Diamonds show cell number. Ten micrograms of CoQ_6 was used as an internal standard. Data are means ± SD of three measurements. Asterisks on bars denote statistically significant differences (** $p<0.01$; * $p<0.05$) relative to YES (3% glucose) (Student's t test).

Fig. 4 Effect of disruption of PKA-related genes on CoQ_{10} production. CoQ_{10} productivity in Δ*git3*, Δ*gpa2*, Δc*yr1*, Δc*gs1*, or Δ*pka1* strains was compared against that of the reference strain PR109. (a) The cAMP/PKA pathway in *S. pombe*. (b) For the pre-culture, the yeast cells were cultivated in 10 mL of YES (3% glucose) medium for 1 day, inoculated at ~1×10^5 cells/mL into 55 mL of YES medium, and then cultivated for 48 hours with rotation at 30°C). CoQ_{10} was extracted and analyzed. Gray bars show CoQ_{10}

693 content per 50 mL of medium, and white bars show CoQ_{10} normalized against cell number.
694 Diamonds show cell number. Ten micrograms of CoQ_6 was used as an internal standard.
695 Data are means ± SD of three measurements. Asterisks on bars denote statistically
696 significant differences (** $p<0.01$; * $p<0.05$) relative to the wild type (Student's t test).
697
698 **Fig. 5** Effect of *rst2* disruption or overexpression on CoQ_{10} production. (a) CoQ_{10}
699 productivity in YMP36 (Δ*pka1*), YMP130 (Δ*rst2*), or YMP220 (Δ*pka1* Δ*rst2*) was
700 compared with that of the reference strain PR109. Strains were grown at 30°C in YES
701 complete liquid medium. Cells were inoculated at 1×10^5 cells/mL and harvested after 48
702 hours of growth. (b) CoQ_{10} productivity in PR110 harboring pREP3X (an empty vector),
703 pREP3X-Rst2 (*nmt1-rst2*), or pREP3X-Rst2 C2H2Δ (*nmt1-rst2* C2H2Δ). For pre-culture,
704 the strains were grown at 30°C in PMU minimal liquid medium with 0.15 μM thiamine.
705 The strains were washed twice with distilled pure water, and then grown at 30°C in PMU
706 minimal liquid medium without thiamine. Cells were inoculated at 1×10^5 cells/mL and
707 harvested after 48 hours of growth. CoQ_{10} was extracted and analyzed. Gray bars show
708 CoQ_{10} content per 50 mL of medium, and white bars show CoQ_{10} normalized against cell
709 number. Diamonds show cell number. Five micrograms of CoQ_6 was used as an internal
710 standard. Data are means ± SD of three measurements. Asterisks on bars denote
711 statistically significant differences (** $p<0.01$; * $p<0.05$) relative to Δ*pka1* (a) or vector
712 control (b) (Student's t test).
713
714 **Fig. 6** Effect of maltose on CoQ_{10} production. CoQ_{10} productivity was tested in YES
715 containing 3% (w/v) maltose (Mal) instead of 3% glucose (Glc) and compared with YES.
716 Cells were grown at 30°C in YES (Glc) complete medium. The pre-culture was washed
717 three times with distilled pure water, and then inoculated at 1×10^5 cells/mL and grown
718 until the indicated time points. CoQ_{10} was extracted and analyzed. Gray bars show CoQ_{10}
719 content per 50 mL of medium, and white bars show CoQ_{10} normalized against cell number.
720 Diamonds show cell number. Five micrograms of CoQ_6 was used as an internal standard.
721 Data are means ± SD of three measurements. (a) Strain PR110. Asterisks on bars denote
722 statistically significant differences (** $p<0.01$; * $p<0.05$) relative to glucose (Student's t
723 test). (b) Strains PR110 (wild type) and YMP179 (Δ*pka1*) were used to compare
724 productivity of CoQ_{10}.
725
726 **Fig. 7** Western blotting for detection of Cdc2, Dlp1, Coq3, Coq4, Coq5, and Coq8. Each
727 sample was subjected to 10.5% SDS–polyacrylamide gel electrophoresis, and analyzed
728 by immunoblotting using rabbit antibodies against Dlp1, Coq3, Coq4, Coq5, and Coq8.

729 Rabbit anti-PSTAIRE antibody (Cdc2) was used as a loading control of whole cell
730 extracts. Horseradish peroxidase–fused anti-rabbit IgG was used as a secondary antibody.
731 Arrows indicate bands corresponding to the target proteins. lane1, PR109 (W. T.); lane2,
732 PR110 (W. T.); lane3, YMP40 (Δ*cgs1*); lane4, YMP177 (Δ*cgs1*); lane5, YMP36 (Δ*pka1*);
733 lane6, YMP179 (Δ*pka1*). Protein bands are indicated at right.
734
735 **Fig. 8** Growth of Δ*pka1* and Δ*cgs1* cells in non-fermentable carbon source media. (a)
736 Growth of the wild type (PR109, open circle), Δ*pka1* (YMP36, open square), or Δ*cgs1*
737 (YMP40, open triangle) in 55 mL of YES medium containing 2% glycerol (w/v) and 1%
738 ethanol (w/v) was monitored by counting cell numbers. Growth of wild type (PR109,
739 closed circle) and Δ*pka1* (YMP36, closed square) cells in YES (which contains 3%
740 glucose) medium is also shown. (b) CoQ_{10} productivity was tested in YES containing 2%
741 glycerol (w/v)/1% ethanol (w/v) or 3% glucose (w/v). (c) CoQ_{10} productivity of YES
742 containing 2% glycerol (w/v)/1% ethanol (w/v) with or without 0.5% casamino acid (w/v)
743 instead of 3% glucose (w/v). The pre-culture was washed three times with distilled pure
744 water, and then inoculated at 1×10^5 cells/mL (a and b) or 1×10^6 cells/mL (c). The cells
745 were harvested at the indicated time points. CoQ_{10} was extracted and analyzed. Gray bars
746 show CoQ_{10} content per 50 mL of medium, and white bars show CoQ_{10} normalized
747 against cell number. Diamonds show cell number. Five micrograms of CoQ_6 was used as
748 an internal standard. Data are means ± SD of three measurements. In panel C, asterisks
749 between bars denote statistically significant differences (** $p<0.01$, * $p<0.05$; Student's
750 t test) relative to wild type (day 4 in glucose). Glc, glucose; Gly, glycerol; EtOH, ethanol;
751 Cas; casamino acid.
752
753

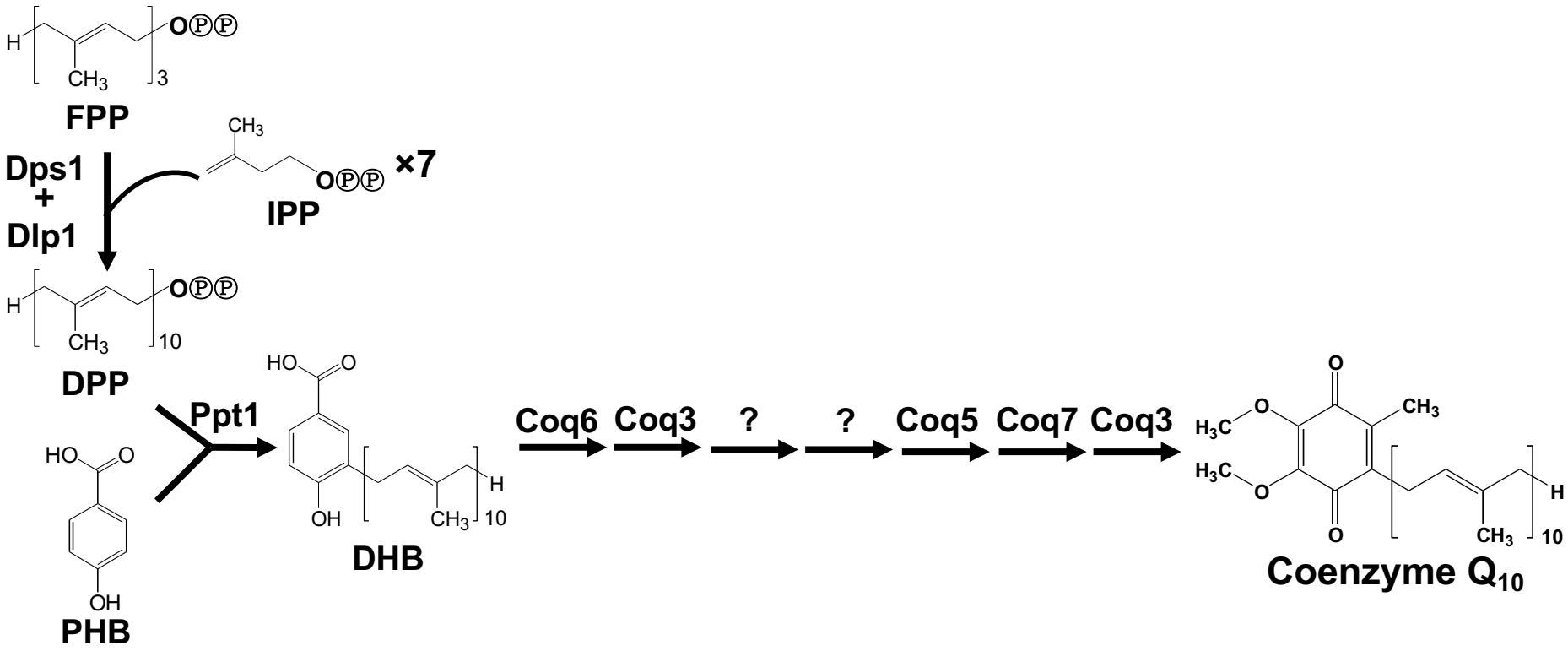
FPP
Dps1
+
Dlp1
IPP
×7
DPP
Ppt1
PHB
DHB
Coq6
Coq3
?
?
Coq5
Coq7
Coq3
Coenzyme Q10

Fig. 1.

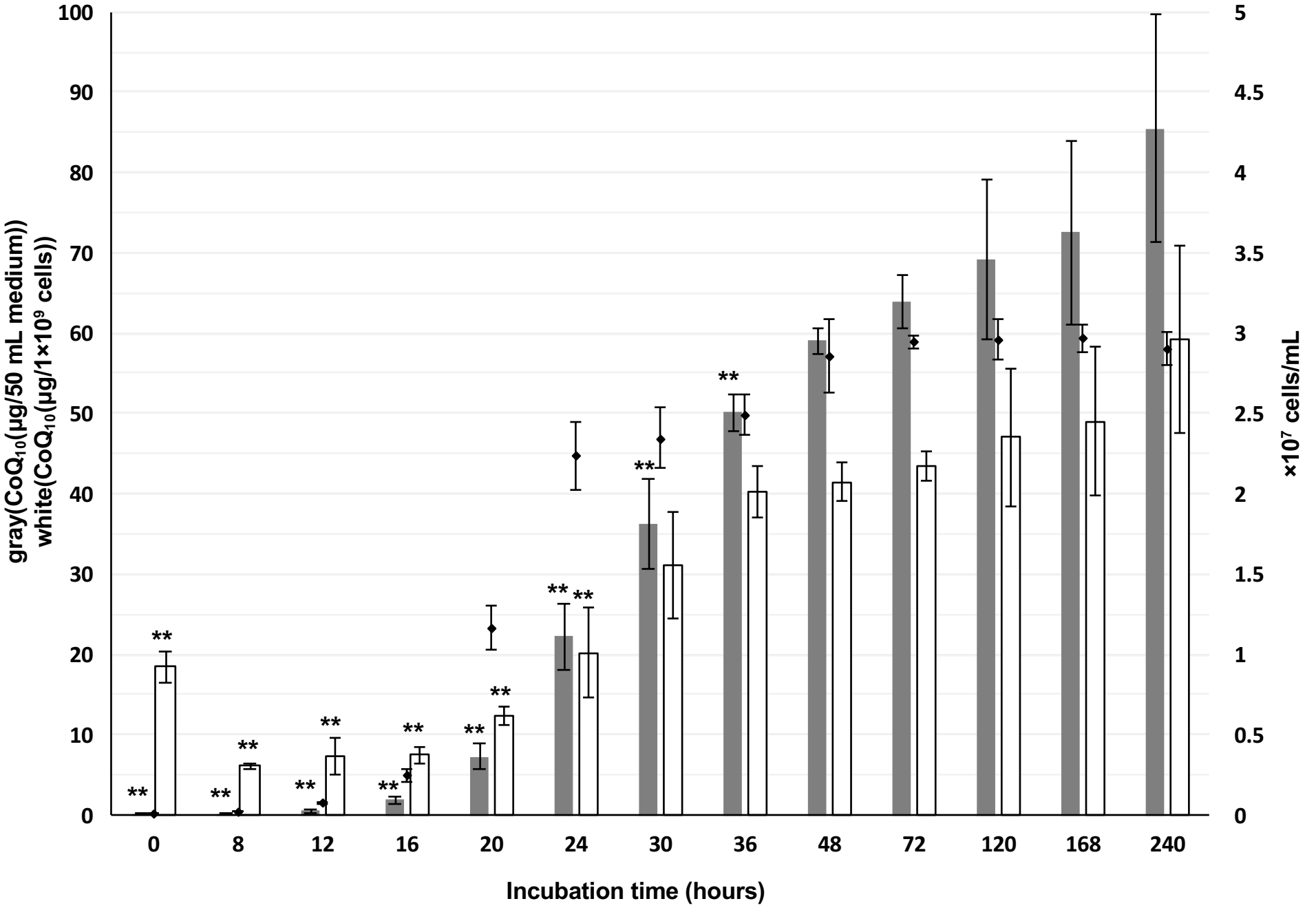
gray(CoQ10(µg/50 mL medium))
white(CoQ10(µg/1×10^9 cells))
×10^7 cells/mL
Incubation time (hours)
0
8
12
16
20
24
30
36
48
72
120
168
240
**

Fig. 2.

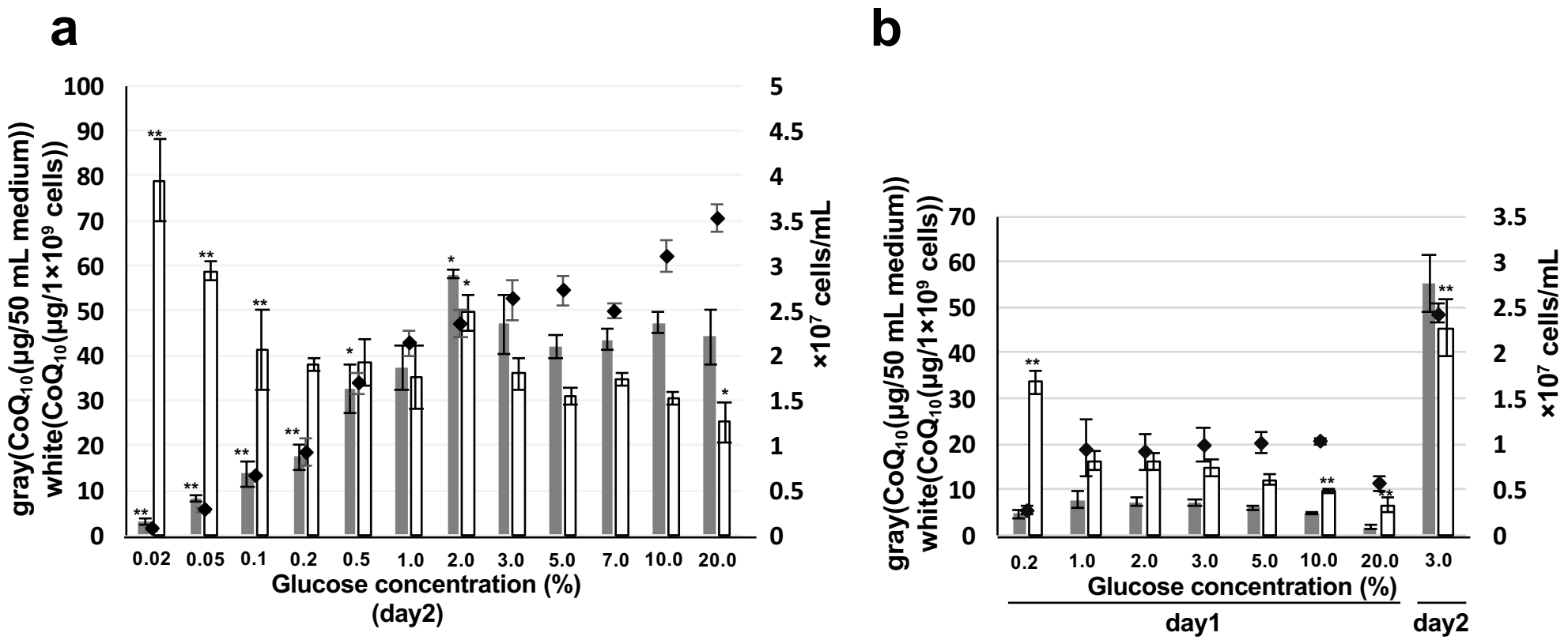
a
gray(CoQ10(μg/50 mL medium))
white(CoQ10(μg/1×10^9 cells))
×10^7 cells/mL
Glucose concentration (%)
(day2)
0.02
0.05
0.1
0.2
0.5
1.0
2.0
3.0
5.0
7.0
10.0
20.0
b
gray(CoQ10(μg/50 mL medium))
white(CoQ10(μg/1×10^9 cells))
×10^7 cells/mL
Glucose concentration (%)
day1
day2

Fig. 3.

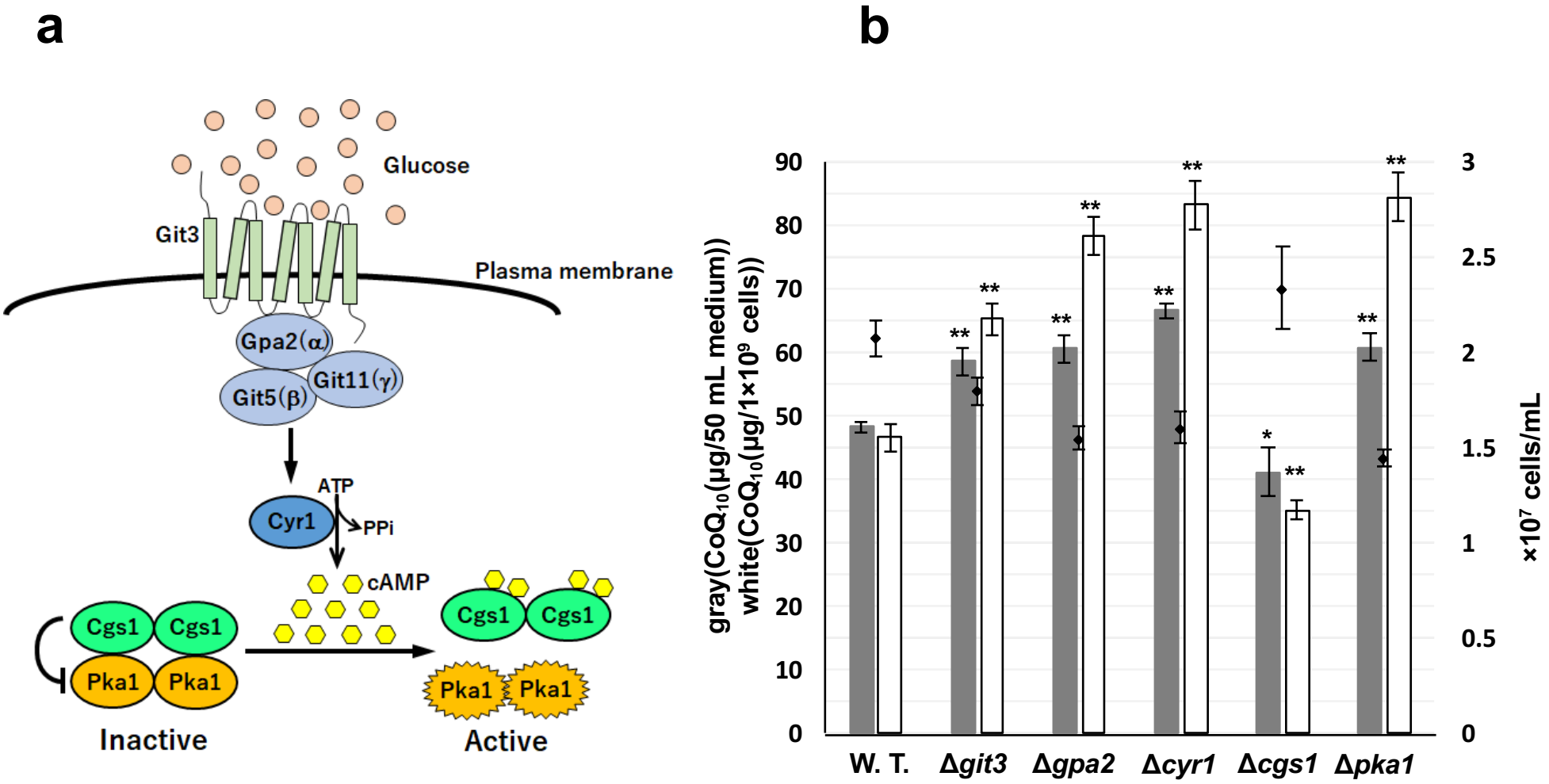
a
Glucose
Git3
Plasma membrane
Gpa2(α)
Git5(β)
Git11(γ)
ATP
Cyr1
PPi
cAMP
Cgs1
Cgs1
Pka1
Pka1
Inactive
Cgs1
Cgs1
Pka1
Pka1
Active
b
gray(CoQ10(μg/50 mL medium))
white(CoQ10(μg/1×10^9 cells))
×10^7 cells/mL
W. T.
Δgit3
Δgpa2
Δcyr1
Δcgs1
Δpka1

Fig. 4.

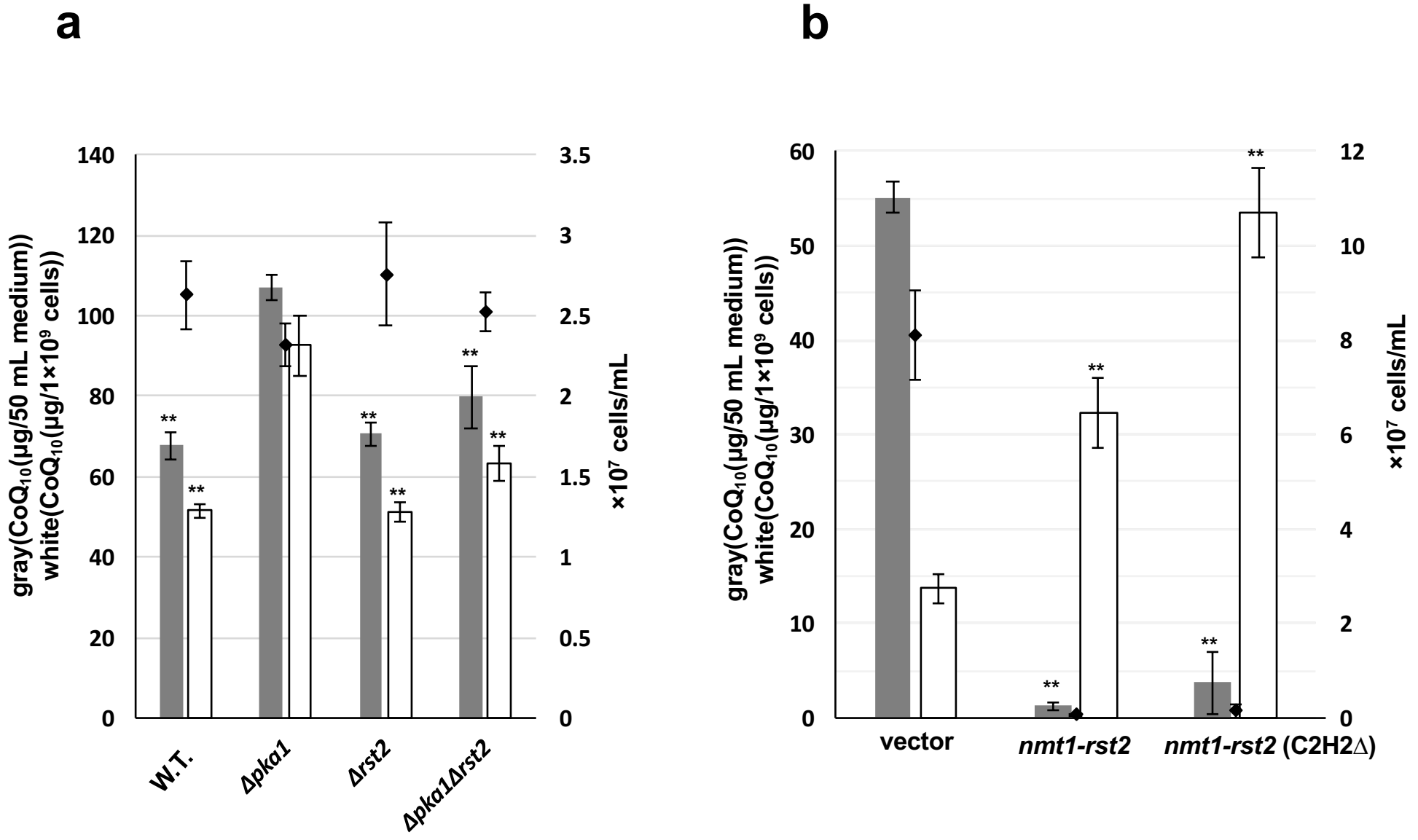
a
b
gray(CoQ10(μg/50 mL medium))
white(CoQ10(μg/1×10^9 cells))
×10^7 cells/mL
W.T.
Δpka1
Δrst2
Δpka1Δrst2
vector
nmt1-rst2
nmt1-rst2 (C2H2△)
**

Fig. 5.

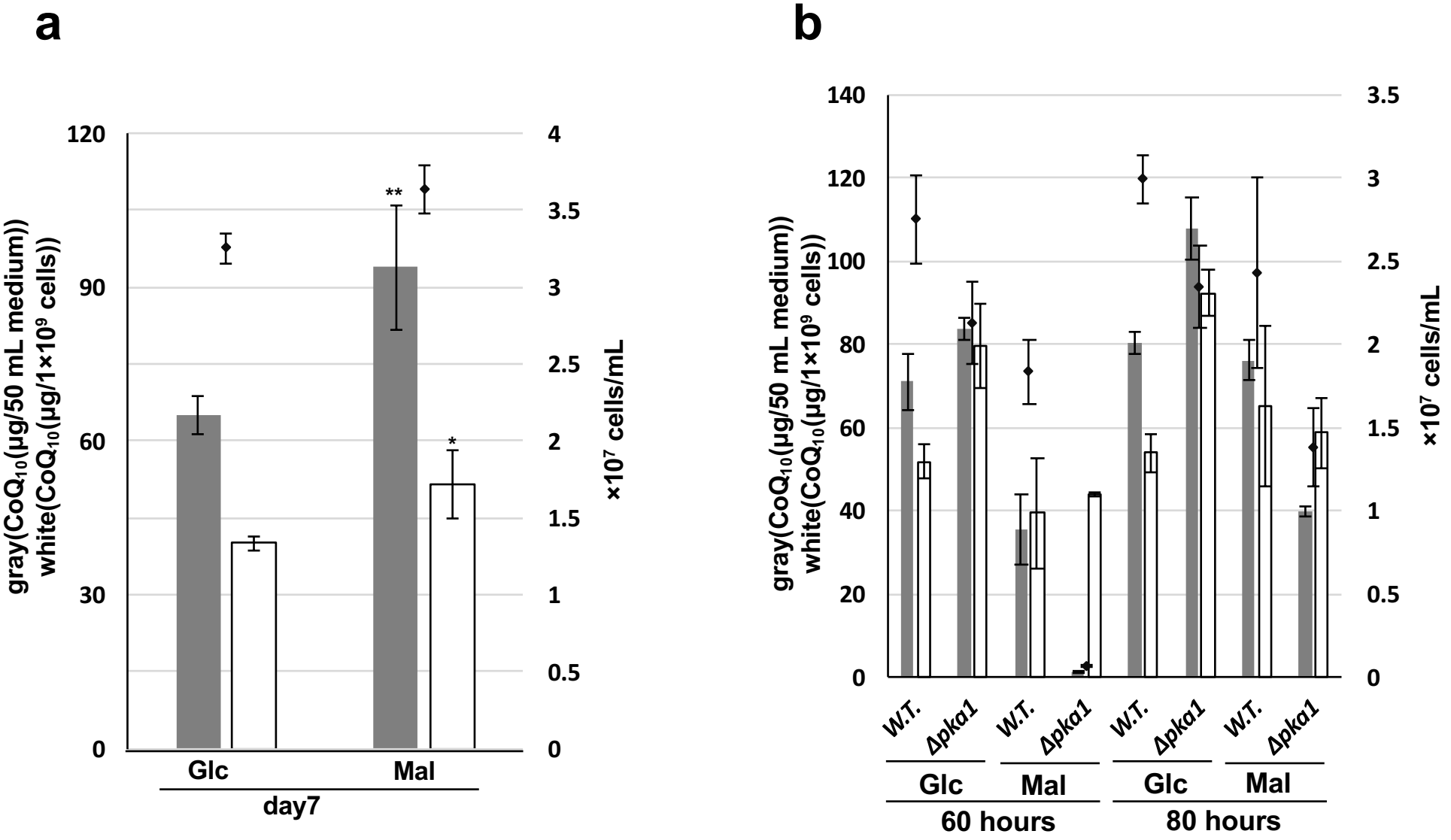
a
120
90
60
30
0
4
3.5
3
2.5
2
1.5
1
0.5
0
**
*
gray(CoQ10(μg/50 mL medium))
white(CoQ10(μg/1×10^9 cells))
×10^7 cells/mL
Glc
Mal
day7
b
140
120
100
80
60
40
20
0
3.5
3
2.5
2
1.5
1
0.5
0
gray(CoQ10(μg/50 mL medium))
white(CoQ10(μg/1×10^9 cells))
×10^7 cells/mL
W.T.
Δpka1
W.T.
Δpka1
W.T.
Δpka1
W.T.
Δpka1
Glc
Mal
Glc
Mal
60 hours
80 hours

Fig. 6.

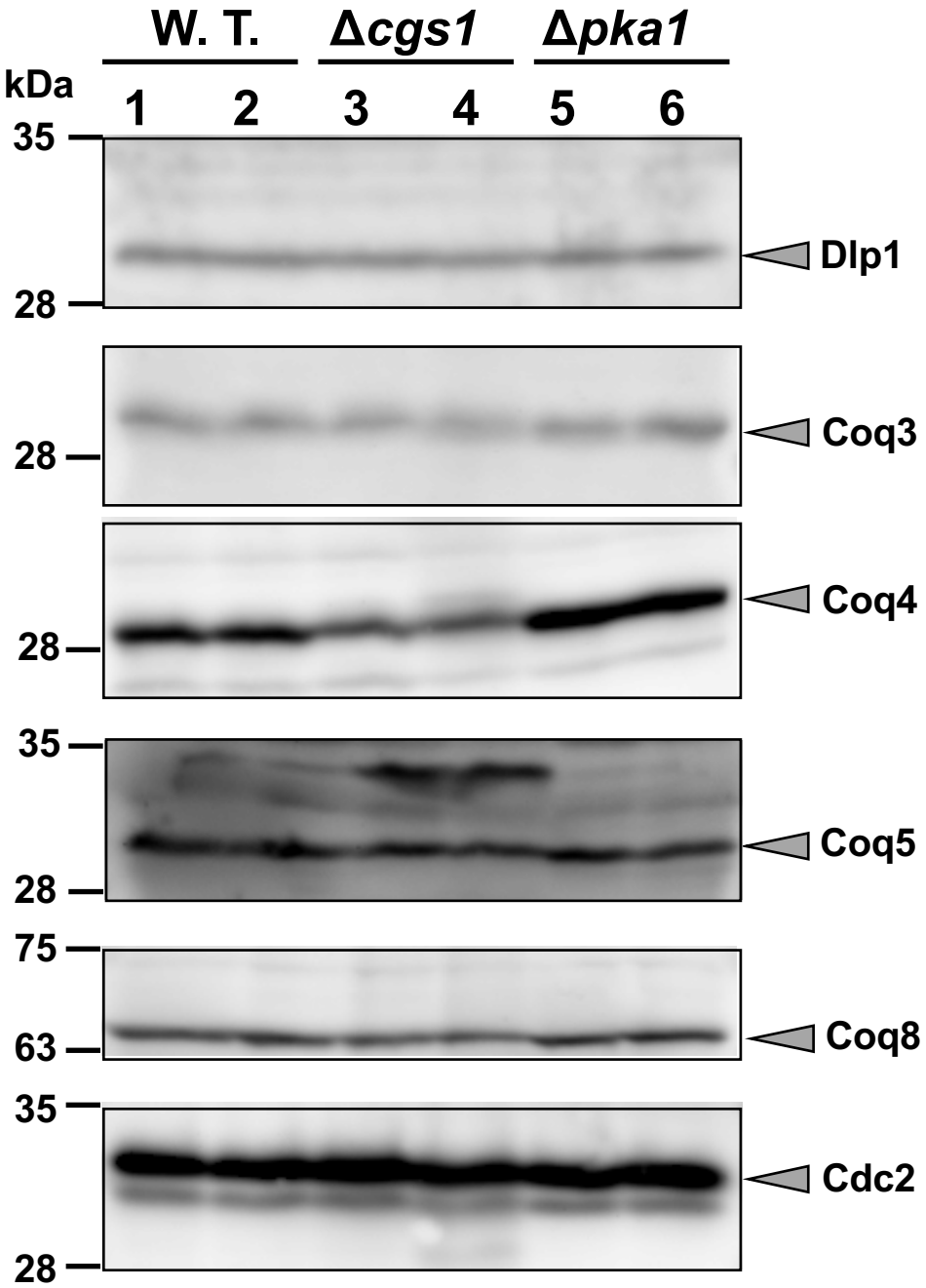
W. T.
Δcgs1
Δpka1
kDa
1
2
3
4
5
6
35
28
Dlp1
28
Coq3
28
Coq4
35
28
Coq5
75
63
Coq8
35
28
Cdc2

Fig. 7.

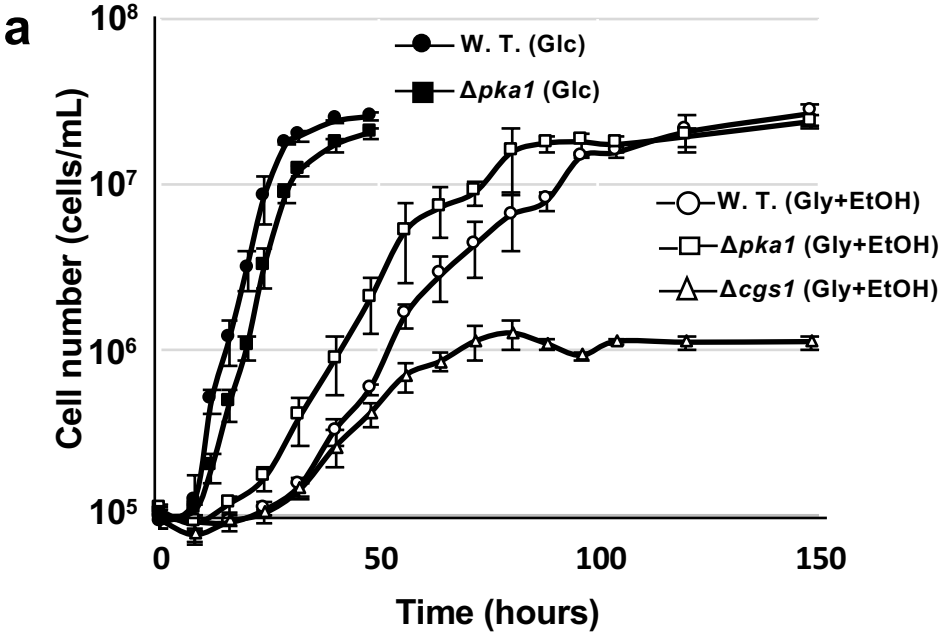
a
Cell number (cells/mL)
Time (hours)
W. T. (Glc)
Δpka1 (Glc)
W. T. (Gly+EtOH)
Δpka1 (Gly+EtOH)
Δcgs1 (Gly+EtOH)

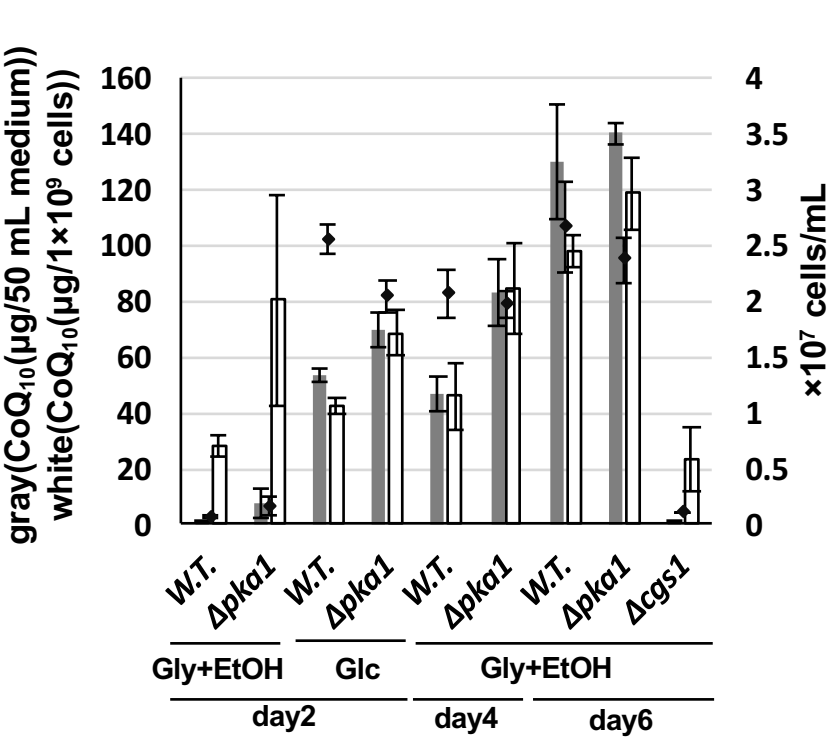
b
gray(CoQ10(μg/50 mL medium))
white(CoQ10(μg/1×10⁹ cells))
×10⁷ cells/mL
W.T.
Δpka1
Δcgs1
Gly+EtOH
Glc
day2
day4
day6

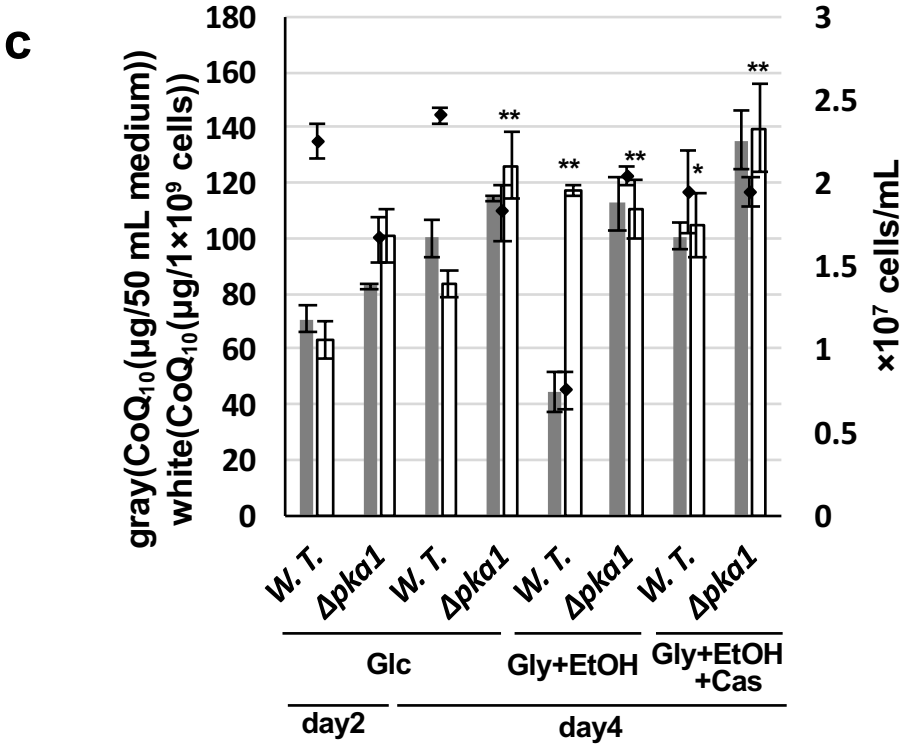
c
gray(CoQ10(μg/50 mL medium))
white(CoQ10(μg/1×10⁹ cells))
×10⁷ cells/mL
W. T.
Δpka1
Glc
Gly+EtOH
Gly+EtOH +Cas
day2
day4

Fig. 8.

Table 1 DNA microarray analyses with wild type, Δ*pka1* and Δ*cgs1*

Upregulated genes inΔ*pka1*

Systematic ID	Gene name	Function	Fold change
SPBPB21E7.01c	*eno102*	enolase (predicted)	27.11
SPCC1739.08c	Unassigned	short chain dehydrogenase (predicted)	20.80
SPBC359.06	*mug14*	adducin	19.74
SPAC22A12.17c	Unassigned	short chain dehydrogenase (predicted)	18.79
SPBC16E9.16c	*lsd90*	Lsd90 protein	15.38
SPAC869.06c	*hry1*	HHE domain cation binding protein (predicted)	15.35
SPAC869.07c	*mel1*	alpha-galactosidase, melibiase	14.19
SPAC22H10.13	*zym1*	metallothionein Zym1	14.14
SPAC869.09	Unassigned	Con-6 family conserved fungal protein	13.01
SPAC1F8.01	*ght3*	hexose transporter Ght3	12.50
SPAC1F8.05	*isp3*	spore wall structural constituent Isp3	11.98
SPBC1289.14	Unassigned	adducin (predicted)	11.97
SPAC23H3.15c	*ddr48*	DNA damage-responsive protein ortholog DDr48	11.69
SPBC1198.14c	*fbp1*	fructose-1,6-bisphosphatase Fbp1	8.13
SPAC637.03	Unassigned	DUF1774 family multi-spanning conserved fungal membrane protein	8.04
SPCC794.04c	Unassigned	amino acid transmembrane transporter (predicted)	7.52
SPCC794.01c	*gcd1*	glucose dehydrogenase Gcd1	7.35
SPAC513.02	Unassigned	phosphoglycerate mutase family	7.20
SPAC139.05	Unassigned	succinate-semialdehyde dehydrogenase (predicted)	6.85
SPCC1795.06	*map2*	P-factor pheromone Map2	6.51
SPAC27D7.03c	*mei2*	RNA-binding protein involved in meiosis Mei2	6.34
SPCC548.07c	*ght1*	hexose transporter Ght1	5.73
SPAC4F8.08	*mug114*	*Schizosaccharomyces pombe* specific protein	5.71
SPAC3G9.11c	*pdc201*	pyruvate decarboxylase (predicted)	5.70
SPBC1683.08	*ght4*	hexose transporter Ght4	5.53
SPAP8A3.04c	*hsp9*	heat shock protein Hsp9	5.52
SPCC338.18	Unassigned	*Schizosaccharomyces pombe* specific protein	5.25
SPAC22F8.05	Unassigned	alpha,alpha-trehalose-phosphate synthase (predicted)	4.67
SPBC8E4.05c	Unassigned	fumarate lyase superfamily	4.67
SPBC56F2.06	*mug147*	*Schizosaccharomyces pombe* specific protein	4.42
SPAC11D3.01c	Unassigned	Con-6 family conserved fungal protein	4.34
SPAC4H3.08	Unassigned	3-hydroxyacyl-CoA dehydrogenase (predicted)	4.33
SPCC757.03c	*hsp3101*	ThiJ domain protein	4.32
SPAC9E9.01	Unassigned	dubious	4.22
SPAC26F1.11	Unassigned	dubious	3.93
SPAC1039.11c	*gto1*	alpha-glucosidase (predicted)	3.88
SPBC947.09	*hsp3103*	ThiJ domain protein	3.81
SPBC365.12c	*ish1*	LEA domain protein	3.70
SPAC977.16c	*dak2*	dihydroxyacetone kinase Dak2	3.69
SPAC5H10.02c	*hsp3102*	ThiJ domain protein	3.67
SPBC21C3.19	*rtc3*	SBDS family protein Rtc3 (predicted)	3.61
SPAC4H3.03c	Unassigned	glucan 1,4-alpha-glucosidase (predicted)	3.60
SPBP4H10.09	*rsv1*	transcription factor Rsv1	3.55
SPAPB24D3.10c	*agl1*	alpha-glucosidase Agl1	3.43
SPBC725.03	Unassigned	pyridoxamine 5'-phosphate oxidase (predicted)	3.42
SPAC11E3.06	*map1*	MADS-box transcription factor Map1	3.41
SPCPB16A4.06c	Unassigned	*Schizosaccharomyces pombe* specific protein	3.39
SPAC869.08	*pcm2*	protein-L-isoaspartate O-methyltransferase Pcm2 (predicted)	3.35
SPBPB21E7.04c	Unassigned	human COMT ortholog 2	3.33
SPAC3C7.13c	Unassigned	glucose-6-phosphate 1-dehydrogenase (predicted)	3.31
SPBC3H7.08c	Unassigned	conserved fungal protein	3.30
SPAC13C5.04	Unassigned	class I glutamine amidotransferase family protein, conserved in fungi, bacteria, plants	3.29
SPAC11D3.18c	Unassigned	carboxylic acid transmembrane transporter (predicted)	3.27
SPCP31B10.06	*mug190*	C2 domain protein	3.27
SPBC24C6.09c	Unassigned	phosphoketolase family protein (predicted)	3.17
SPCC965.06	*osr2*	potassium channel subunit/aldo-keto reductase (predicted)	3.17
SPBPB2B2.12c	*gal10*	UDP-glucose 4-epimerase/aldose 1-epimerase Gal10	3.08
SPAC2F3.05c	Unassigned	xylose and arabinose reductase (predicted)	3.03
SPAPJ691.02	Unassigned	yippee-like protein	3.00
SPAC13F5.03c	*gld1*	mitochondrial glycerol dehydrogenase Gld1	2.96
SPAC22F3.12c	*rgs1*	regulator of G-protein signaling Rgs1	2.84
SPBC1773.06c	*adh8*	alcohol dehydrogenase (predicted)	2.77
SPCC162.10	*ppk33*	serine/threonine protein kinase Ppk33 (predicted)	2.76
SPAC23C11.06c	Unassigned	vacuolar membrane hydrolase	2.75
SPAC4F10.17	Unassigned	conserved fungal protein	2.73
SPACUNK4.17	Unassigned	NAD binding dehydrogenase family protein, human DHDH ortholog	2.70
SPBC32F12.03c	*gpx1*	glutathione peroxidase Gpx1	2.70
SPCC16A11.15c	Unassigned	*Schizosaccharomyces* specific protein	2.69
SPAC30D11.01c	*gto2*	alpha-glucosidase (predicted)	2.64
SPAC15A10.05c	*mug182*	NADHX epimerase (predicted)	2.57
SPBC32C12.02	*ste11*	transcription factor Ste11	2.54
SPAC13F5.07c	*hpz2*	zf PARP type zinc finger protein Hpz2	2.53
SPBC1105.14	*rsv2*	transcription factor Rsv2	2.53
SPAPB1A11.03	Unassigned	cytochrome b2 (L-lactate cytochrome-c oxidoreductase) (predicted)	2.53
SPAPB1A10.14	*pof15*	F-box protein (predicted)	2.51
SPBP4H10.10	*rbd3*	mitochondrial rhomboid family protease	2.50
SPAC869.03c	Unassigned	urea transporter (predicted)	2.50
SPAC3C7.05c	*mug191*	alpha-1,6- mannanase (predicted)	2.50
SPAC32A11.02c	Unassigned	DUF4449 family conserved fungal protein	2.50
SPAC1565.04c	*ste4*	adaptor protein Ste4	2.48
SPBC1683.09c	*frp1*	ferric-chelate reductase Frp1	2.48
SPAC4D7.02c	*pgc1*	phosphatidylglycerol phospholipase C Pgc1 (predicted)	2.47
SPAC869.05c	Unassigned	sulfate transporter (predicted)	2.46
SPBC3D6.16	Unassigned	dubious	2.43
SPBC19C7.04c	Unassigned	DUF2406 family conserved fungal protein	2.42
SPAC5H10.01	*dgc1*	mitochondrial D-glutamate cyclase Dgc1 (predicted)	2.36
SPCC338.12	*pbi2*	proteinase B inhibitor Pbi2 (predicted)	2.35
SPBC4.01	*dni2*	tetraspan protein Dni2 (predicted)	2.33
SPAC19G12.09	Unassigned	NADH/NADPH dependent indole-3-acetaldehyde reductase	2.29
SPBC24C6.06	*gpa1*	G-protein alpha subunit	2.29

Upregulated genes in Δ *pka1* (continued)

Systematic ID	Gene name	Function	Fold change
SPAC15E1.02c	Unassigned	DUF1761 family protein	2.28
SPBC19C2.04c	*ubp11*	ubiquitin C-terminal hydrolase Ubp11	2.26
SPBC1604.01	*egt1*	Ergothioneine biosynthesis protein Egt1	2.23
SPAC23E2.03c	*ste7*	meiotic suppressor protein Ste7	2.21
SPAC513.06c	*dhd1*	D-xylose 1-dehydrogenase (NADP+) (predicted)	2.21
SPBC1685.05	*htr11*	serine protease (predicted)	2.21
SPCC4G3.03	Unassigned	WD40/YVTN repeat-like protein	2.20
SPCC417.15	Unassigned	dubious	2.17
SPAC26F1.04c	*etr1*	enoyl-[acyl-carrier protein] reductase (predicted)	2.17
SPAC20H4.11c	*rho5*	Rho family GTPase Rho5	2.16
SPAC2E1P3.01	Unassigned	dehydrogenase (predicted)	2.15
SPBC1773.05c	*tms1*	hexitol dehydrogenase (predicted)	2.14
SPBC11C11.06c	Unassigned	*Schizosaccharomyces* specific protein	2.14
SPCC191.01	Unassigned	*Schizosaccharomyces* specific protein	2.10
SPAC29A4.17c	Unassigned	mitochondrial FUN14 family protein	2.08
SPAC688.04c	*gst3*	glutathione S-transferase Gst3	2.05
SPAC688.03c	Unassigned	human AMMECR1 homolog	2.03
SPAC3F10.10c	*map3*	pheromone M-factor receptor Map3	2.03
SPAC8C9.03	*cgs1*	cAMP-dependent protein kinase regulatory subunit Cgs1	2.03
SPAC26F1.14c	*aif1*	apoptosis-inducing factor homolog Aif1 (predicted)	2.03
SPAC3C7.02c	*pil2*	meiotic eisosome BAR domain protein Pil2	2.02
SPBP4H10.12	Unassigned	protein with a role in ER insertion of tail-anchored membrane proteins (predicted)	2.00

Downregulated genes in Δ *pka1*

Systematic ID	Gene name	Function	Fold change
SPAC186.05c	*gdt1*	Golgi calcium and manganese antiporter Gdt1	0.09
SPAC1039.02	Unassigned	extracellular 5'-nucleotidase, human NT5E family (predicted)	0.10
SPBPB21E7.07	*aes1*	enhancer of RNA-mediated gene silencing	0.13
SPBPB2B2.01	Unassigned	amino acid transmembrane transporter (predicted)	0.13
SPBC1271.07c	Unassigned	N-acetyltransferase (predicted)	0.15
SPBPB10D8.01	Unassigned	cysteine transporter (predicted)	0.19
SPBC428.11	*met17*	homocysteine synthase Met17	0.20
SPBPB2B2.05	Unassigned	class I glutamine amidotransferase family protein	0.23
SPCC330.03c	Unassigned	NADPH-hemoprotein reductase (predicted)	0.25
SPBPB2B2.06c	Unassigned	extracellular 5'-nucleotidase, human NT5E family (predicted)	0.26
SPAC5H10.03	Unassigned	phosphoglycerate mutase family	0.29
SPBCPT2R1.08c	*tlh2*	RecQ type DNA helicase Tlh1	0.30
SPAC212.11a	*tlh1*	RecQ type DNA helicase	0.30
SPAC11D3.03c	Unassigned	aminomethyltransferase-like and DUF1989 family protein	0.32
SPAC977.01	*ftm1*	sub-telomeric 5Tm protein family Ftm1	0.33
SPAC750.05c	*ftm4*	sub-telomeric 5Tm protein family Ftm4	0.33
SPBC1348.02	*ftm5*	sub-telomeric 5Tm protein family Ftm5	0.34
SPAC11D3.02c	Unassigned	ELLA family acetyltransferase (predicted)	0.34
SPBC947.04	*pfl3*	cell surface glycoprotein (predicted), DIPSY family	0.34
SPAC56F8.12	Unassigned	DUF2434 family conserved fungal multispanning membrane protein	0.35
SPAC5H10.06c	*adh4*	alcohol dehydrogenase Adh4	0.37
SPAC1F8.06	*fta5*	cell surface glycoprotein	0.39
SPBC1861.02	*abp2*	ARS binding protein Abp2	0.39
SPCC594.03	Unassigned	*Schizosaccharomyces* specific protein	0.40
SPBC4C3.03	*thr1*	homoserine kinase Thr1 (predicted)	0.40
SPAC328.09	Unassigned	mitochondrial 2-oxoadipate and 2-oxoglutarate transporter (predicted)	0.42
SPAC750.03c	Unassigned	methyltransferase (predicted)	0.43
SPBC1198.02	*dea2*	adenine deaminase Dea2	0.43
SPBC8E4.03	Unassigned	agmatinase 2 (predicted)	0.43
SPBP8B7.01c	*pop7*	RNAseP RNAse MRP subunit Pop7 (predicted)	0.43
SPCC1682.09c	*gcg1*	mitochondrial guanine nucleotide transporter Gcs1 (predicted)	0.43
SPAC186.01	*pfl9*	cell surface glycoprotein (predicted), DIPSY family	0.44
SPAC186.09	*pdc102*	pyruvate decarboxylase (predicted)	0.44
SPCC1672.03c	*gud1*	guanine deaminase Gud1 (predicted)	0.45
SPAC977.03	Unassigned	methyltransferase (predicted)	0.46
SPBC1711.05	*srp40*	nucleocytoplasmic transport chaperone Srp40 (predicted)	0.46
SPAC5H10.10	Unassigned	NADPH dehydrogenase, (Old yellow enzyme) involved in small alpha,beta-unsaturated carbonyl compounds (predicted)	0.47
SPCC1682.08c	*mpf2*	meiotic pumilio family RNA-binding protein Mpf2	0.48
SPAC6F6.11c	Unassigned	pyridoxine-pyridoxal-pyridoxamine kinase (predicted)	0.49
SPAC26F1.05	*mug106*	*Schizosaccharomyces* specific protein	0.49
SPBPB2B2.18	Unassigned	conserved fungal plasma membrane protein	0.49
SPBP4G3.02	*pho1*	acid phosphatase Pho1	0.49

Upregulated genes in Δ *cgs1*

Systematic ID	Gene name	Function	Fold change
SPBPB2B2.18	Unassigned	conserved fungal plasma membrane protein	4.83
SPCC737.04	Unassigned	*S. pombe* specific UPF0300 family protein 6	2.58
SPBC19C7.04c	Unassigned	DUF2406 family conserved fungal protein	2.18
SPCC417.06c	*mug27*	meiosis specific protein kinase Mug27/Slk1	2.11
SPAC869.01	Unassigned	hydrolase activity, implicated in cellular detoxification (predicted)	2.05
SPAC212.02	Unassigned	*Schizosaccharomyces* specific protein	2.04

Downregulated genes in Δ *cgs1*

Systematic ID	Gene name	Function	Fold change
SPAC27D7.03c	*mei2*	RNA-binding protein involved in meiosis Mei2	0.42
SPAC1F8.06	*fta5*	cell surface glycoprotein	0.47
SPAC186.01	*pfl9*	cell surface glycoprotein (predicted), DIPSY family	0.49

Table 2. CoQ_{10} production under various conditions

Condition	Strain	CoQ_{10} (μg)	CoQ_{10} (μg)/10^9 cells	CoQ_{10} (mg)/g-DCW	mg-DCW
3%Glc 1day	PR110	3.3 ±1.0	10.7 ±1.7	0.183 ±0.029	17.7 ±3.8
	YMP179	1.8 ±0.5	29.0 ±3.8	0.174 ±0.010	10.0 ±2.1
3%Glc 2days	PR110	48.5 ±4.1	33.9 ±2.4	0.610 ±0.053	79.8 ±7.8
	YMP179	54.2 ±2.3	56.3 ±6.4	0.650 ±0.007	83.5 ±3.0
3%Glc 5days	PR110	68.7 ±2.5	41.4 ±2.8	0.688 ±0.070	100.7 ±13.1
	YMP179	91.0 ±17.1	49.2 ±13.1	0.643 ±0.038	141.0 ±20.3
3%Glc 7days	PR110	65.1 ±3.8	40.0 ±1.4	0.618 ±0.027	105.3 ±3.7
10%Glc 7days	PR110	89.8 ±10.4	48.3 ±7.1	0.953 ±0.117	94.3 ±1.9
3%Mal 7days	PR110	93.8 ±12.0	51.7 ±6.6	0.643 ±0.061	145.8 ±10.5
0.02%Glc 2days	PR110	3.1 ±0.4	67.9 ±4.0	0.438 ±0.031	7.0 ±0.4
3%Glc 2days	PR110	31.2 ±0.9	36.5 ±1.8	0.570 ±0.027	54.7 ±1.3
3%Glc 4days*	PR110	69.2 ±2.6	45.3 ±1.1	0.802 ±0.086	86.8 ±8.3
	YMP179	108.1 ±5.3	91.6 ±6.5	0.957 ±0.054	113.0 ±3.8
2%Gly+1%EtOH +0.5%Cas 4days*	PR110	72.5 ±15.3	80.8 ±5.7	0.920 ±0.049	78.5 ±13.7
	YMP179	100.5 ±5.2	175.5 ±10.8	0.984 ±0.021	102.1 ±4.9

Note: The starting cell number of main culture is $1x10^5$ cells/ml.
CoQ_{10} (μg) denotes CoQ_{10} amount contained in 50 ml of each medium.
* indicates 10^6 cells/ml inoculation.

Supplemental materials

Applied Microbiology and Biotechnology

CoQ_{10} production in *Schizosaccharomyces pombe* is increased by reduction of glucose levels or deletion of *pka1*

Ikuhisa Nishida[1], Kazumasa Yokomi[1], Kouji Hosono[1], Kazuhiro Hayashi[1], Yasuhiro Matsuo[1, 2], Tomohiro Kaino[1, 2], & Makoto Kawamukai[1, 2]

[1]Department of Life Sciences, Faculty of Life and Environmental Sciences, Shimane University, 1060 Nishikawatsu, Matsue 690-8504, Japan.
[2]Institute of Agricultural and Life Sciences, Academic Assembly, Shimane University, 1060 Nishikawatsu, Matsue 690-8504, Japan.

Corresponding author: Makoto Kawamukai:
E-mail:kawamuka@life.shimane-u.ac.jp.

Telephone/Fax: 81-852-32-6587, Fax: 81-852-32-6092.

Table S1 Yeast strains used in this study

Strain	Genotype	Source
JZ633	*h^{90} leu1-32 ura4-D18 pka1::ura4*	H. Kunimoto et al., 2000
PR109	*h^{-} leu1-32 ura4-D18*	P. Russell
PR110	*h^{+} leu1-32 ura4-D18*	P. Russell
RM19	*h^{+} leu1-32 ura4-D18 dlp1::kanMX6*	R. Miki et al., 2008
KH3 (RM2)	*h^{+} leu1-32 ura4-D18 coq3::kanMX6*	K. Hayashi et al., 2014
KH4 (LV974)	*h^{+} leu1-32 ura4-D18 coq4::kanMX6*	K. Hayashi et al., 2014
KH5 (RM7)	*h^{+} leu1-32 ura4-D18 coq5::kanMX6*	R. Miki et al., 2008
KH8 (OG2)	*h^{+} leu1-32 ura4-D18 coq8::kanMX6*	K. Hayashi et al., 2014
YMP28	*h^{-} leu1-32 ura4-D18 cyr1::ura4*	Y. Matsuo and M. Kawamukai, 2017
YMP36	*h^{-} leu1-32 ura4-D18 pka1::ura4*	Y. Matsuo and M. Kawamukai, 2017
YMP37	*h^{+} leu1-32 ura4-D18 pka1::ura4*	Lab stock
YMP39	*h^{-} leu1-32 ura4-D18 gpa2::ura4*	Y. Matsuo and M. Kawamukai, 2017
YMP40	*h^{-} leu1-32 ura4-D18 cgs1::ura4*	Y. Matsuo and M. Kawamukai, 2017
YMP41	*h^{+} leu1-32 ura4-D18 cgs1::ura4*	Lab stock
YMP43	*h^{+} leu1-32 ura4-D18 git3::ura4*	Y. Matsuo and M. Kawamukai, 2017
YMP130	*h^{-} leu1-32 ura4-D18 rst2::kanMX6*	K. Takenaka et al., 2018
YMP131	*h^{+} leu1-32 ura4-D18 rst2::kanMX6*	Lab stock
YMP177	*h^{+} leu1-32, ura4-D18 cgs1::natMX6*	Lab stock
YMP179	*h^{+} leu1-32, ura4-D18 pka1::natMX6*	Lab stock
YMP201	*h^{-} leu1-32 ura4-D18 rst2::natMX6*	Lab stock
YMP220	*h^{-} leu1-32 ura4-D18 pka1::ura4 rst2::natMX6*	Lab stock

Table S2. Kinase gene deletion mutants used in this study

Strains name	Genotype	Product
MBY1747-2	/CC1322.12::ura4 (bub1)	serine/threonine protein kinase
MBY1748	/CC74.03C::ura4 (ssp2)	serine/threonine protein kinase
MBY1749	/CC63.08::ura4 (atg1)	autophagy and CVT pathway serine/threonine protein kinase
MBY1750	/CC417.06c::ura4 (mug27)	meiosis specific protein kinase
MBY1751	/CC24B10.07::ura4 (gad8)	AGC family protein kinase
MBY1753	/CC1020.10::ura4 (oca2)	serine/threonine protein kinase
MBY1754	/BC8D2.01::ura4 (gsk31)	serine/threonine protein kinase
MBY1755	/BC725.06c::ura4 (ppk31)	serine/threonine protein kinase
MBY1756	/BC6B1.02::ura4 (ppk30)	Ark1/Prk1 family protein kinase
MBY1757	/BC557.04::ura4 (ppk29)	Ark1/Prk1 family protein kinase
MBY1758	/BC337.04::ura4 (ppk27)	serine/threonine protein kinase
MBY1759	/BC32C2.03c::ura4 (ppk25)	serine/threonine protein kinase
MBY1760	/BCBC21.07c::ura4 (ppk24)	serine/threonine protein kinase
MBY1761	/BC18H10.15::ura4 (ppk23)	serine/threonine protein kinase
MBY1762	/BC1861.09::ura4 (ppk22)	serine/threonine protein kinase
MBY1763	/BC16E9.13::ura4 (ksp1)	serine/threonine protein kinase
MBY1764	/BC119.07::ura4 (ppk19)	serine/threonine protein kinase
MBY1765	/AC890.03::ura4 (ppk16)	serine/threonine protein kinase
MBY1766	/AC4G8.05::ura4 (ppk14)	serine/threonine protein kinase
MBY1767	/AC3H1.13::ura4 (ppk13)	serine/threonine protein kinase
MBY1768	/AC2F3.15::ura4 (lsk1)	P-TEFb-associated cyclin-dependent protein kinase
MBY1769	/AC2C4.14c::ura4 (ppk11)	PAK-related kinase
MBY1770	/AC29A4.16::ura4 (hal4)	halotolerence protein 4
MBY1771	/AC23H4.17c::ura4 (srb10)	cyclin-dependent protein Srb mediator subunit kinase
MBY1772	/AC23H4.02::ura4 (ppk9)	serine/threonine protein kinase
MBY1773	/AC22G7.08::ura4 (ppk8)	serine/threonine protein kinase
MBY1774	/AC22E12.14c::ura4 (sck2)	serine/threonine protein kinase
MBY1775	/AC222.07c::ura4 (hri2)	eIF2 alpha kinase
MBY1776	/AC20G4.03c::ura4 (hri1)	eIF2 alpha kinase
MBY1777	/AC823.03::ura4 (ppk15)	serine/threonine protein kinase
MBY1778	/AC1D4.11c::ura4 (lkh1)	dual specificity protein kinase
MBY1779	/AC15A10.13::ura4 (ppk3)	HEAT repeat protein
MBY1780	/AC12B10.14c::ura4 (ppk2)	serine/threonine protein kinase
MBY1781	/AC167.01::ura4 (ire1)	serine/threonine protein kinase Ppk4/ sensor for unfolded proteins in the ER
MBY1782	/CC162.10::ura4 (ppk33)	serine/threonine protein kinase
MBY1783	/CC1322.08::ura4 (srk1)	MAPK-activated protein kinase
MBY1784	/AC9G1.02::ura4 (wis4)	MAP kinase kinase kinase
MBY1785	/BC21C3.18::ura4 (spo4)	serine/threonine protein kinase
MBY1786	/AC1F5.09c::ura4 (shk2)	PAK-related kinase
MBY1787	/BC106.10::ura4 (pka1)	cAMP-dependent protein kinase catalytic subunit
MBY1789	/BC8D2.19::ura4 (mde3)	serine/threonine protein kinase, meiotic
MBY1790	/AC23C4.12::ura4 (hhp2)	serine/threonine protein kinase
MBY1791	/AC23A1.06c::ura4 (cmk2)	MAPK-activated protein kinase
MBY1792	/CC1259.13::ura4 (chk1)	Chk1 protein kinase
MBY1793	/BC1D7.05::ura4 (byr2)	MAP kinase kinase kinase
MBY1795	/BC119.08::ura4 (pmk1)	MAP kinase
MBY1796	/AC2F7.03c::ura4 (pom1)	DYRK family protein kinase
MBY1797	/BC1271.16c::ura4 (mph1)	dual specificity protein kinase
MBY1798	/CC74.06::ura4 (mak3)	histidine kinase
MBY1799	/BC3H7.15::ura4 (hhp1)	serine/threonine protein kinase
MBY1800	/ACUNK12.02::ura4 (cmk1)	calcium/calmodulin-dependent protein kinase
MBY1801	/CC1450.11c::ura4 (cek1)	serine/threonine protein kinase
MBY1802	/AC1D4.13::ura4 (byr1)	MAP kinase kinase
MBY1803	/CC18B5.03::ura4 (wee1)	M phase inhibitor protein kinase
MBY1805	/AC3C7.06c::ura4 (pit1)	serine/threonine protein kinase, meiotic
MBY1806	/AC1F3.02c::ura4 (mkh1)	MEK kinase (MEKK)
MBY1807	/AC27E2.09::ura4 (mak2)	histidine kinase
MBY1808	/AC19E9.02::ura4 (fin1)	serine/threonine protein kinase, NIMA related
MBY1809	/AC1805.05::ura4 (cki3)	serine/threonine protein kinase
MBY1810	/CC18B5.11c::ura4 (cds1)	replication checkpoint kinase
MBY1811	/AC24B11.06::ura4 (sty1)	MAP kinase
MBY1812	/AC1687.15::ura4 (gsk3)	serine/threonine protein kinase
MBY1813	/BC12D12.04c::ura4 (pck2)	protein kinase C (PKC)-like
MBY1814	/BC660.14::ura4 (mik1)	mitotic inhibitor kinase
MBY1815	/AC1834.08::ura4 (mak1)	histidine kinase
MBY1816	/BC530.14c::ura4 (dsk1)	SR protein-specific kinase
MBY1817	/BC1347.06c::ura4 (cki1)	serine/threonine protein kinase
MBY1818	/AC57A10.02::ura4 (cdr2)	serine/threonine protein kinase
MBY1820	/CC297.03::ura4 (ssp1)	serine/threonine protein kinase
MBY1821	/BC543.07::ura4 (pek1)	MAP kinase kinase
MBY1822	/CC4G3.08::ura4 (psk1)	serine/threonine protein kinase
MBY1823	/AC14C4.03::ura4 (mek1)	Cds1/Rad53/Chk2 family protein kinase
MBY1825	/AC1D4.06c::ura4 (csk1)	cyclin-dependent kinase activating kinase
MBY1826	/AC644.06c::ura4 (cdr1)	NIM1 family serine/threonine protein kinase
MBY1827	/AC16C9.07::ura4 (pom2)	serine/threonine protein kinase
MBY1828	/BC1778.10c::ura4 (ppk21)	serine/threonine protein kinase
MBY1830	/CP1E11.02::ura4 (ppk38)	Ark1/Prk1 family protein kinase
MBY1831	/AC140.05::ura4 (ppk1)	serine/threonine protein kinase
MBY1832	/APJ736.02c::ura4 (ppk6)	serine/threonine protein kinase
MBY1836	/BP35G2.05c::ura4 (cki2)	serine/threonine protein kinase
MBY1837	/CC16C4.11::ura4 (pef1)	Pho85/PhoA-like cyclin-dependent kinase
MBY1838	/BC216.05::ura4 (rad3)	ATR checkpoint kinase
MBY1840	/BC336.14c::ura4 (ppk26)	serine/threonine protein kinase, PAN complex subunit
MBY1841	/CC1919.03c::ura4 (amk2)	AMP-activated protein kinase beta subunit
MBY1842	/AC1006.09::ura4 (win1)	MAP kinase kinase kinase
MBY1844	/BP23A10.10::ura4 (ppk32)	serine/threonine protein kinase
MBY1845	/AC17G8.14c::ura4 (pck1)	protein kinase C (PKC)-like

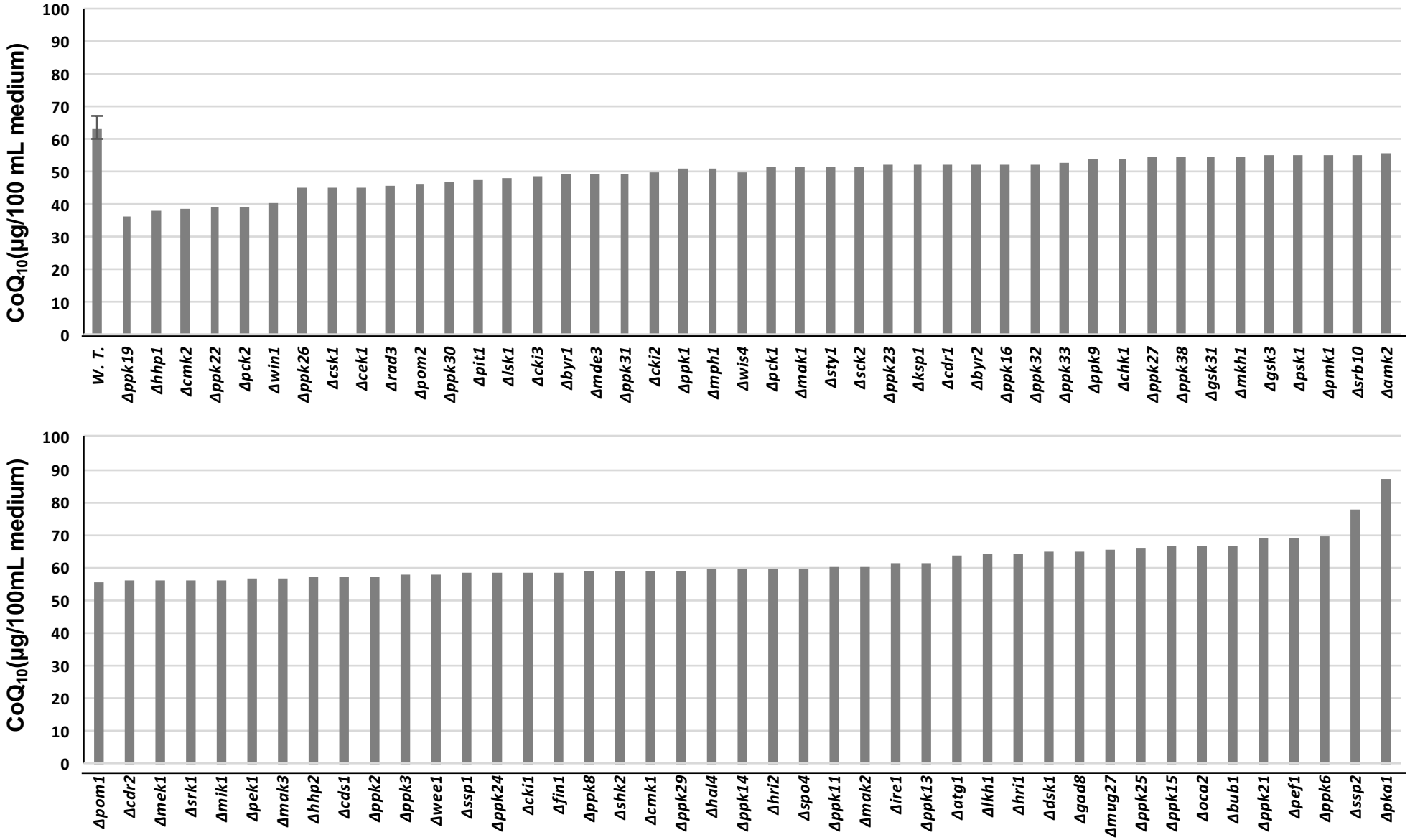

Fig. S1 Effect of kinase gene disruption on CoQ_{10} production. CoQ_{10} productivity in 87 kinase gene disruptants was compared with that of the reference strain PR109. Strains were grown at 30°C in YES complete medium. The pre-culture was inoculated at 1×10^5 cells/mL and harvested after 48 hours growth. CoQ_{10} was extracted and analyzed. Bars represent CoQ_{10} content normalized against cell number (μg/100 mL/1×10^9 cells). For the wild type, data are represented as means ± SD of four measurements.

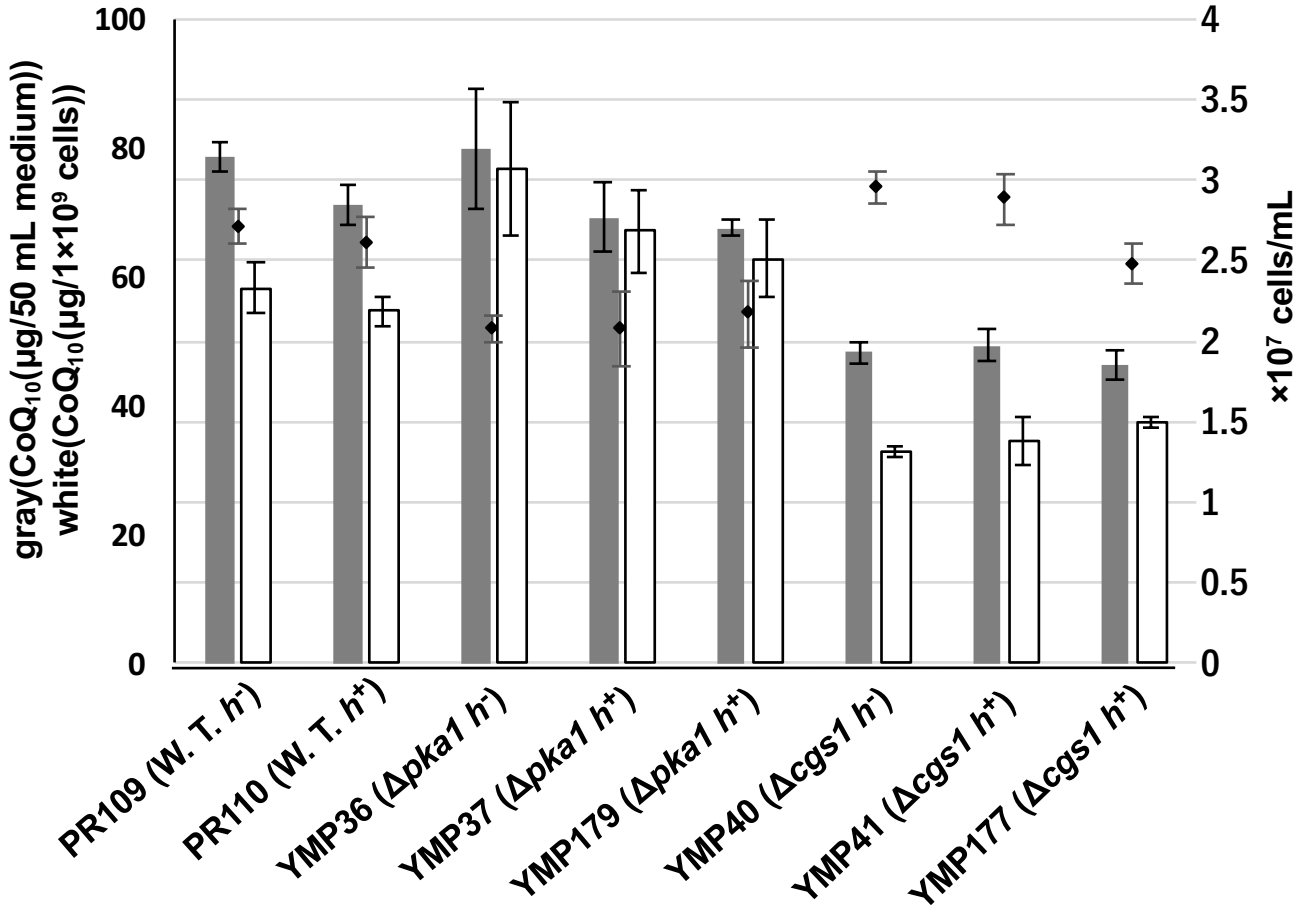

Fig. S2 Evaluation of CoQ_{10} production in various *pka1* and *cgs1* disruptants. CoQ_{10} productivity was compared between Δc*gs1* or Δ*pka1* and the wild type strains (PR109 and PR110). Experimental conditions were similar to those in Fig. 4b. Data are means ± SD of three or four measurements. Asterisks on bars denote statistically significant differences (** $p<0.01$, * $p\leq0.05$) relative to parental strain (Student's t test).

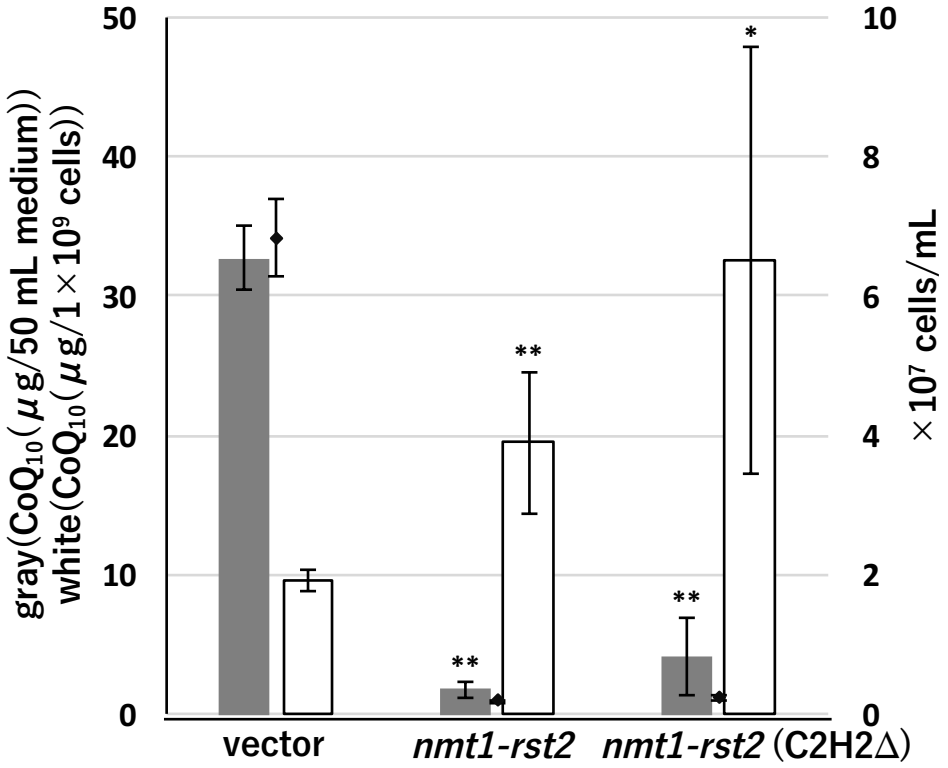

Fig. S3 Effect of *rst2* overexpression on CoQ_{10} production. CoQ_{10} productivity in PR110 harboring pREP3x (an empty vector), pREP3x-Rst2 (*nmt1-rst2*), or pREP3x-Rst2 C2H2Δ (*nmt1-rst2* C2H2Δ). The experimental procedure is similar to that of Fig. 5b. Media were inoculated at 1×10^6 cells/mL and harvested after 24 hours growth. Asterisks on bars denote statistically significant differences (** $p<0.01$; * $p<0.05$) relative to the vector control (Student's t test).

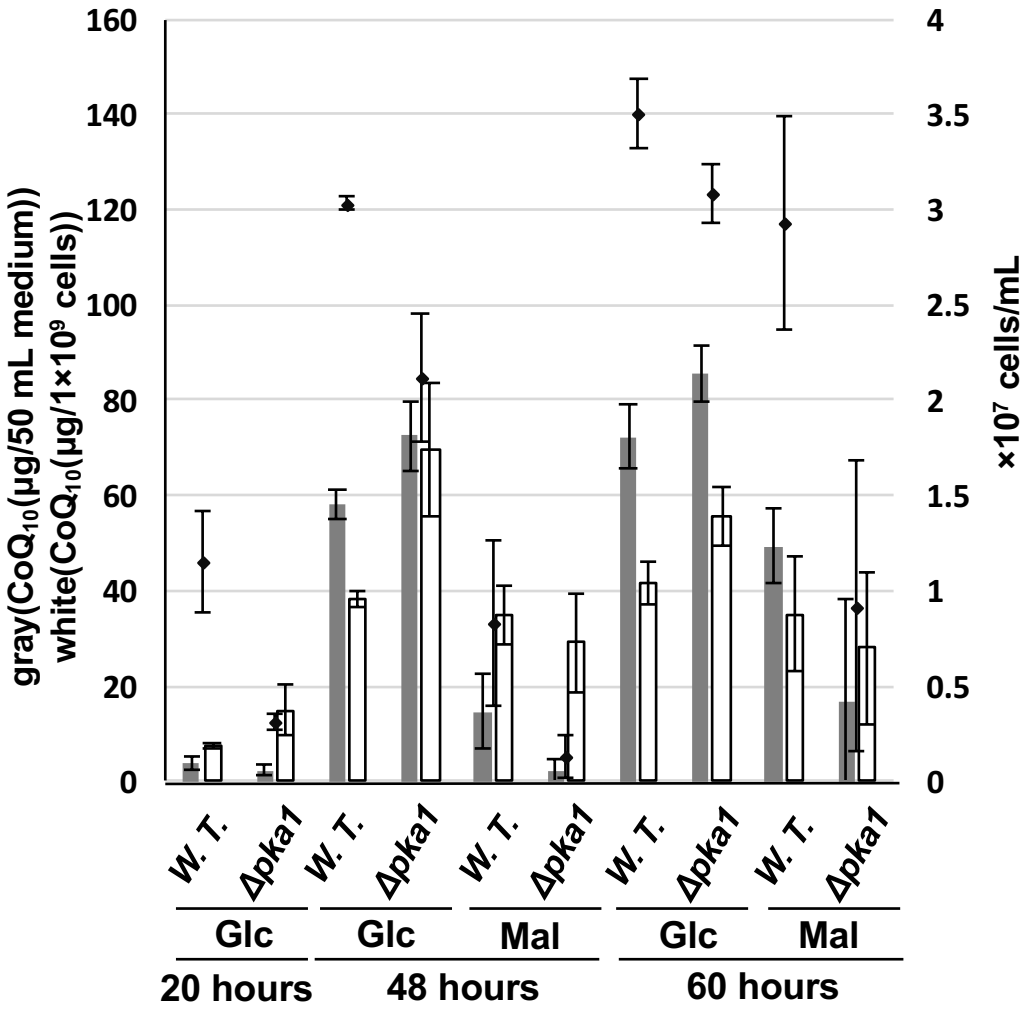

Fig. S4 Effect of shorter incubations in maltose on CoQ_{10} production. CoQ_{10} productivity was tested in YES containing 3% maltose (w/v) with a shorter incubation time. The experimental conditions were similar to those in Fig. 6b.

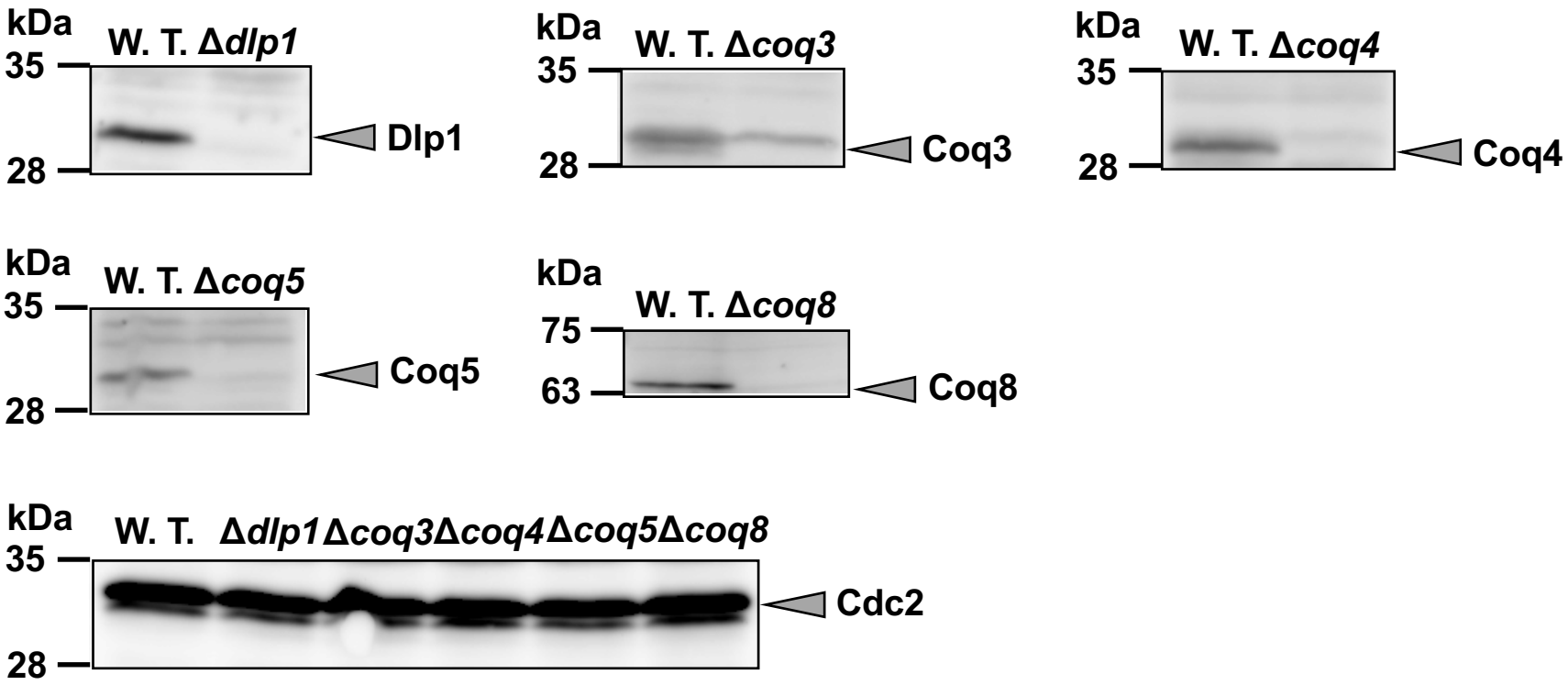

Fig. S5 Western blotting for detection of Cdc2, Dlp1, Coq3, Coq4, Coq5, and Coq8. Each sample was subjected to 10.5% SDS–polyacrylamide gel electrophoresis, and analyzed by immunoblotting using rabbit antibodies against Dlp1, Coq3, Coq4, Coq5, and Coq8. Rabbit anti-PSTAIRE antibody (Cdc2) was used as a loading control of whole cell extracts. Horseradish peroxidase–fused anti-rabbit IgG was used as a secondary antibody. Arrows indicate bands corresponding to the target proteins. PR110 (W. T.); RM19 (Δ*dlp1*); RM2 (Δ*coq3*); LV974 (Δ*coq4*); RM7 (Δ*coq5*); OG2 (Δ*coq8*). Protein bands are indicated at right.

Fig. S5.

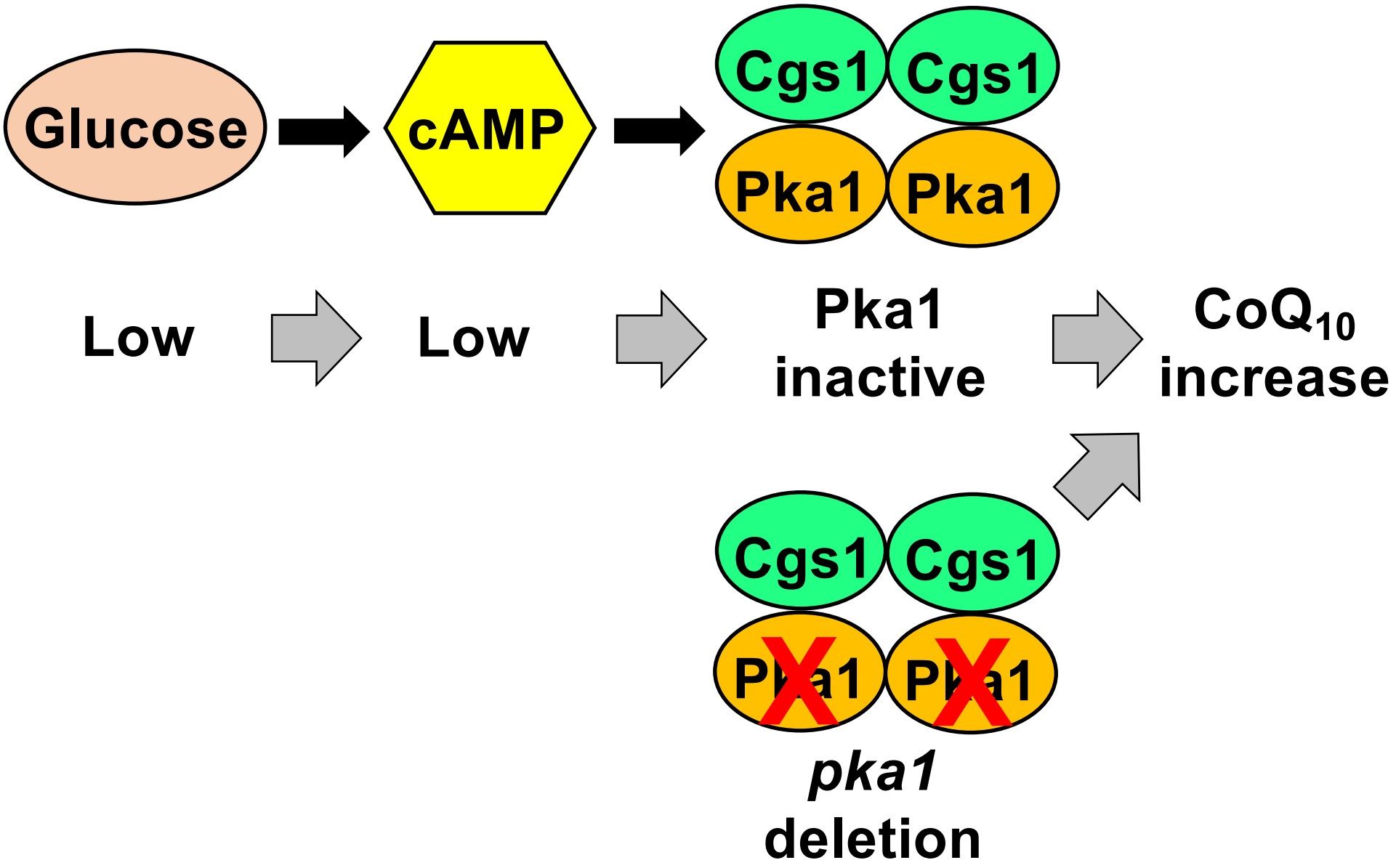

Fig. S6 Model: How cAMP/PKA signaling affects production of CoQ_{10}. When glucose levels decrease, the synthesis of cAMP declines due to lack of activation of adenylyl cyclase. When cAMP levels are low, PKA is inactive due to formation of a complex between its catalytic subunit (Pka1) and regulatory subunit (Cgs1). Under low-glucose conditions or following deletion of the *pka1* gene, CoQ_{10} is produced at high levels.